



Trend analysis of temperature, rainfall, and reference evapotranspiration for Ludhiana district of Indian Punjab using non-parametric statistical methods

Mahesh Chand Singh¹ · Sanjay Satpute¹ · Vishnu Prasad² · Krishan Kumar Sharma³

Received: 29 June 2021 / Accepted: 12 January 2022 / Published online: 28 January 2022
© Saudi Society for Geosciences 2022

Abstract

Climate change, which is one of the main determinants of agricultural production, has started affecting the pattern of crop growth, productivity, and quality of produce from the last few couple of decades in various agro-climatic zones globally. Any change in climatic factors such as temperature, evapotranspiration (ET), and rainfall is bound to have a significant impact on agricultural production. Thus, climate monitoring, trend analysis, and model-based prediction are highly significant to mitigate the climate change impacts on crop growth patterns, production, and quality traits. A study was thus undertaken at Punjab Agricultural University, Ludhiana, India, to (1) estimate reference evapotranspiration (ET_o) using $FAO-ET_o$ calculator; (2) study and detect trend in long-term (1970–2019) recorded temperature (T_{min} and T_{max}), rainfall and ET_o using Mann–Kendall's test, Sen's slope test, standard normal homogeneity test (SNHT), and Pettitt's test in XLSTAT software; (3) study correlation of ET_o with T_{min} , T_{max} , and rainfall; and (4) develop regression models for estimating ET_o on seasonal and annual basis. All the tests indicated a significant trend in T_{min} (increasing) and ET_o (decreasing) during all seasons (spring, summer, autumn, and winter), as well as on annual basis at 5% level of significance, whereas no trend was recorded in T_{max} and rainfall data. The SNHT and Pettitt's test confirmed the existence of a change-point in both ET_o and T_{min} data for all seasons as well as on annual basis. Both Mann–Kendall's and homogeneity tests indicated no trend or change point in T_{max} (except a change-point during spring) and rainfall data. The positive correlation of ET_o with T_{max} , wind speed (v_w), and sunshine hours (SSH) formed an increasing trend in ET_o with increase in these variables and vice-versa. The negative correlation of ET_o with relative humidity (RH_{min} and RH_{max}), rainfall, and T_{min} indicated a decreasing trend in ET_o . The study offers a basis to predict the futuristic climate scenarios in the region for planning crops and manage irrigation to mitigate the climate change impacts on agricultural production. The statistical comparison indicated that the developed models were sufficiently accurate and would be useful in simplified estimation of ET_o on seasonal and annual basis for the study region.

Keywords Ludhiana · Mann–Kendall test · Modeling · Reference evapotranspiration (ET_o) · Sen's slope · Trend analysis

Introduction

Climate change, resulting from natural processes and anthropogenic forces, is negatively affecting the water resources (hydrology), crop water requirements, and therefore the agricultural production globally (Zhang et al. 2009; IPCC 2014). The extreme events such as floods and droughts are the example of negative impacts of climate change (IPCC 2014; Surendran et al. 2014; Akinsanola and Zhou 2019; Gbode et al. 2019). The continuous change in climate scenarios is resulting in increased temperature, particularly the minimum temperature (Singh 2016). The increase in average global temperature may significantly increase the evaporation and land-surface drying (IPCC 2014), subsequently

Responsible Editor: Zhihua Zhang

✉ Mahesh Chand Singh
msrawat@pau.edu

- ¹ Department of Soil and Water Engineering, Punjab Agricultural University, Ludhiana 141004, Punjab, India
- ² Water Technology Centre, Indian Agricultural Research Institute, New Delhi 110012, India
- ³ Regional Research Station, Ballawal Saunkhri, Punjab Agricultural University, Ludhiana 144521, Punjab, India

increasing the probability of drought occurrence (Dai et al. 2004). FAO (2001) has reported about 15–35% reduction of crop yields in Africa and West Asia, with increase in mean temperature from 2.0 to 4.0 °C, whereas about 25–35% reduction in the Middle East. Thus, a continuous monitoring and trend analysis of climatic parameters such as temperature and evapotranspiration (ET) with change point detection becomes significant (Vincent et al. 2015) for better management of water resources. Trend analysis of hydrological and climatic variables is frequently carried out to quantify the effect of climate change on future agricultural production (Jain et al. 2013; Suryavanshi et al. 2014; Kishore et al. 2016; Malik et al. 2020; Saadi et al. 2019).

For carrying out trend analysis of time-series data and change point detection, non-parametric statistical approaches can be used, to investigate whether there exists a trend in a long-term dataset or it follows any distribution at a fixed significance level. The change detection test of time-series data is done for reduction in uncertainty in climate information (Jaiswal and Lohani 2015). The non-parametric tests such as Mann–Kendall trend test (Mann 1945; Kendall 1975), Sen's slope test (Sen 1968), SNHT (Alexandersson 1986; Gonzalez-Rouco et al. 2001; Stepanek et al. 2009), Pettitt's test (Pettitt 1979; Mauget 2003), and Buishand's range test (Buishand 1982) are widely used for detection of trend and change-point in the time-series parameters such as temperature, humidity, rainfall, sunshine hours, wind speed, and ET (Salarijazi et al. 2012; Emmanuel et al. 2019; Ajayi and Ilori 2020). The recent studies involving trend analysis and change-point detection in long-term time series data using Mann Kendall's test include Malik et al. (2019), Bannayan et al. (2020), Elzopy et al. (2020), Ilori and Ajayi (2020), and Sharma et al. (2020) for temperature and rainfall, Sharma et al. (2020) for relative humidity and solar radiation, and Mohsin and Lone (2021), Ndiaye et al. (2020), and Sharma et al. (2020) for reference evapotranspiration (ET_0).

Any significant change in evapotranspiration (ET_0 or ET_c) in relation to different meteorological parameters, mainly the temperature (T_{max} and T_{min}) and rainfall (Sharafi and Mir Karim 2020), is bound to have a significant impact on agricultural water management, crop growth, and the productivity. ET from agricultural fields (Penman 1948), which represents the water loss through evaporation from soil surface and transpiration from plant leaves (Chattopadhyay and Hulme 1997), significantly affects the crop productivity. On the basis of previous studies, it may be concluded that ET increases with increase in global temperature. However, numerous studies have reported decreasing trend of ET in some of the regions. In this context, Chattopadhyay and Hulme (1997) have reported decreased ET_0 with increased temperature in India, mainly due to increase in relative humidity (RH) and reduction in solar radiation.

Moreover, Bandyopadhyay et al. (2009) have admitted a declining trend of ET_0 throughout India. ET is affected by several climatic variables, including temperature and rainfall distribution. Increasing temperature and decreasing rainfall may significantly enhance the ET (ET_0 and actual or crop ET , i.e., ET_c) and reduce the yields of various crops (Lobell et al. 2008). Thus, precise estimation of ET_0 , followed by computation ET_c , can play a great role in management of available water resources (Zhang, et al. 2015), crop planning (Shuttleworth and Wallace 2009), and therefore the agricultural water, particularly in the water scarce regions globally. Several methods (empirical, water balance-based, and physical approaches) are available for estimating ET_0 , which require temperature (max. and min.), relative humidity (max. and min.), sunshine hours, and wind velocity as inputs (Peterson et al. 1995; Irmak et al. 2012; Sun et al. 2016). Any significant change (decrease or increase) in these climatic parameters is likely to have a significant change (decrease or increase) in ET_0 . FAO- ET_0 calculator is one of the tools for accurate estimation of ET_0 , using the above listed climatic parameters as input.

Previously, Hundal and Kaur (2002a) have declared a steady increase of about of 0.07 °C per year in the minimum air temperature in the present studied region over of period of 30 years (between 1970 and 2002). Hundal et al. (1997) reported an increasing rainfall trend over normal for both annual and kharif season for the past 30 years at Ludhiana. Further, Gill et al. (2010) reported rainfall below normal for 24 years for Ludhiana being highest (1334 mm) during 1988 and lowest (379.6 mm) during 1974. Furthermore, Hundal and Kaur (2002b) have recorded about 150 mm increment in rainfall over a period of 30 years for the same region. Furthermore, the average decadal minimum and maximum temperatures are expected to increase by 29.1 and 12.8%, respectively, by the end of the twenty-first century in the region (Singh 2016), with a significant reduction (13.2%) in average decadal rainfall (Singh 2016).

At present, more than 85% area in the study region is under agriculture with net irrigated area of about 98% and having a cropping intensity of more than 190%. Out of the total area under irrigation, about 72.50% area is irrigated with groundwater (> 14 lakh tube wells in operation), whereas only 27.50% area is irrigated with surface water supplied through canals (Singh 2019). Due to the more reliance on groundwater, followed by its over-exploitation, the depth to water table in the region falls in the range of 20–40 mbgl (Singh 2019). Thus, the injudicious surface irrigation water policies and excessive ground water pumping are the key reasons for acute depletion of the groundwater resources in the region. Furthermore, the rice–wheat crop rotation in

relation to uncontrolled water flooding has encouraged the water table depletion (about 70 cm/year) during few couple of decades (Gulati et al. 2017). Besides, the average annual rainfall in the region is decreasing and erratic in nature, which fails to contribute significantly to the crop water requirement. Thus, the water management particularly for major field crops of the region is highly needed in relation to irrigation scheduling and saving of water to be applied. This can be achieved by various techniques, one of which is the study of crop evapotranspiration, which is taken equivalent to crop water requirement. The trend analysis of ET_0 may help in better understanding of the crop water requirements in relation to climate change impacts (Dinpathoh and Babamiri 2020).

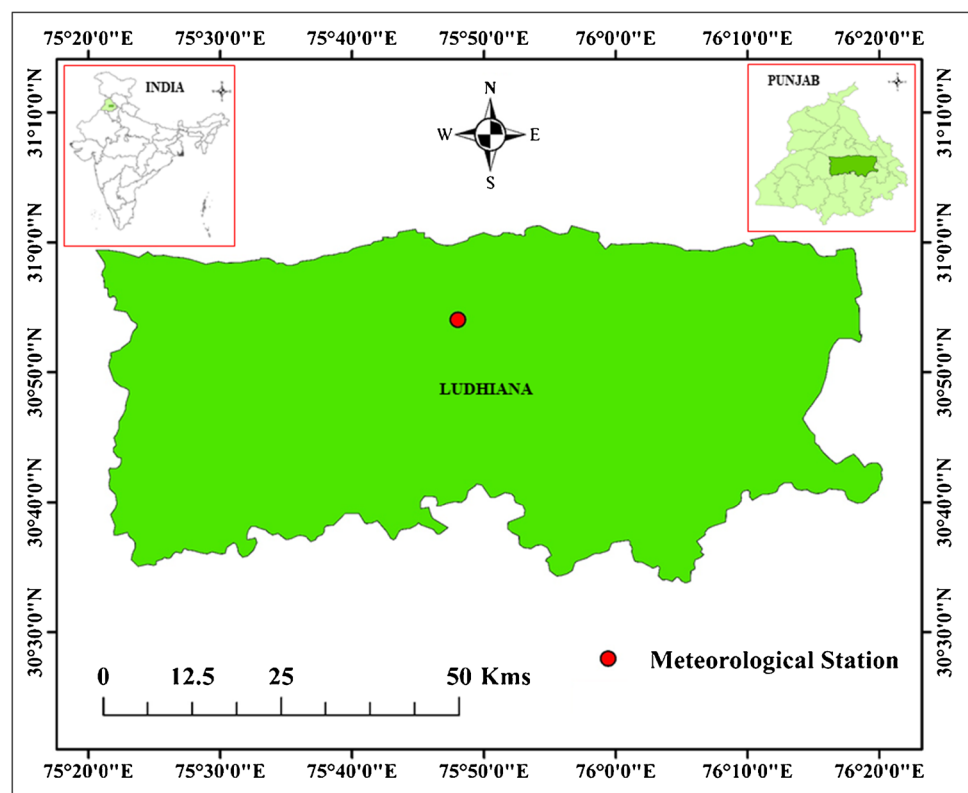
Keeping the this information in observance, the present study was undertaken to (1) estimate ET_0 using *FAO-ET₀* calculator; (2) study and detect trend in long-term (1970–2019) recorded temperature (minimum and maximum), rainfall and estimated ET_0 using Mann–Kendall’s trend test, Sen’s slope test, standard normal homogeneity test (SNHT), and Pettitt’s test; (3) study correlation of ET_0 with T_{\min} , T_{\max} , and rainfall using correlation test in XLSTAT software; and (4) develop regression models for easy prediction of ET_0 on seasonal as well as annual basis for the present study region.

Materials and methods

Description of study area

The present investigation was carried out in the Department of Soil and Water Engineering, Punjab Agricultural University (PAU), Ludhiana. The study site is located between 30° 54' N (latitude) and 75° 48' E (longitude) at an elevation of 247.0 m above the mean sea level. Figure 1 demonstrates the study area map. The study region is characterized as semi-arid with sub-tropical climatic conditions, resulting in very hot summer (April to June) and cold winters (December to January). The mean temperatures (max. and min.) indicate variations throughout the year. The temperature during summer exceeds 38 °C, even touches 47 °C. During winter (December and January), frost is experienced, and the minimum temperature drops below 4.0 °C. North-Eastern winds dominate in the region during this period. The mean annual rainfall of the study region is 680 mm, and about 75–80% of it is received in the months of June to September. In winter, only a few showers of rains (cyclonic) are experienced through western disturbances. There are mainly four different seasons in the study region, viz., spring, March–May (pleasant); summer, June–August (warm); autumn, September–October (mild cold); and winter, November–February (extreme cold).

Fig. 1 Study area map



Data collection

The daily climatic data for 50 years (1970–2019) was obtained from the meteorological observatory of Punjab Agricultural University (PAU), Ludhiana. The climatic data included temperature (minimum and maximum), relative humidity (minimum and maximum), wind speed, sunshine hours, and rainfall.

Methodology for trend analysis

Trend is a significant change (either positive or negative) in a random variable with respect to time, which can be measured using statistical tests (parametric or non-parametric). *FAO-ET_o* calculator was used for estimation of daily reference evapotranspiration (*ET_o*). Trend analysis (trend and change-point detection) was carried out for estimated daily *ET_o*, temperature (minimum and maximum), and rainfall using non-parametric tests, viz., Mann–Kendall’s trend test (Kendall 1975), Sen’s slope test (Sen 1968), SNHT test (Alexandersson 1986), and Pettitt’s test (Pettitt 1979). The estimated *ET_o* and recorded data was transformed to monthly basis. The resulting data then divided into four seasons, viz., spring (March–May), summer (June–August), autumn (September–November), and winter (December–February). The analysis was carried out on seasonal as well as annual basis using XLSTAT software. The estimated daily *ET_o* was also converted to monthly and then seasonal basis. Correlation test was also performed for testing the relationship between estimated *ET_o*, temperature (*T_{max}* and *T_{min}*), and rainfall.

Mann–Kendall test

The Mann–Kendall (Mann 1945; Kendall 1948) test is one of the most commonly used non-parametric tests for detection of trends in long-term hydro-meteorological time-series data of climate (Bandyopadhyay et al. 2009; Liang et al. 2010; Tabari et al. 2011; Azizzadeh and Javan 2015; Rahmani et al. 2015; Diop et al. 2018; Bodian et al. 2020), as it does not necessitate the data to follow any of the statistical distributions (Diop et al. 2015). Moreover, it is not sensitive to the extreme values (Shadmani et al. 2012). The test interpretation criteria is based on rejection or acceptance of two hypotheses, viz., null hypothesis (*H₀*), i.e., there is no trend in the series, and the alternate hypothesis (*H_a*), i.e., reject *H₀*, indicating existence of trend in the time series data. If *p* value is less than alpha (α), i.e., 0.05, one should accept *H_a*, which indicates existence of a trend in the time-series data (hydrological or climatic data). However, if the *p* value is more than α , one cannot reject *H₀*, which indicates that there exists no trend in the data series.

The formula for Mann–Kendall’s statistical *S* is expressed by Eq. 1. The mean of *S* is 0. The downward or upward

trend is indicated by the sign of *Z* value (negative or positive), which can be obtained using the variance of *S*, as given below (Eq. 3). For $n > 10$, *Z* follows nearly a normal distribution and can be computed using Eq. 4 (Hirsch and Slack 1984) as reported in Ndiaye et al. (2020).

$$S = \sum_{j=1}^{j=n-1} \sum_{i=j+1}^{i=n} \text{sign}(x_i - x_j) \tag{1}$$

where x_i = value of the variable at time *i*, x_j = value of the variable at time *j*, n = length of the series, and $\text{sign}()$ = a function as described below as expressed by Eq. 2.

$$\text{sign}(x_i - x_j) = \begin{cases} 1 \text{ if } (x_i - x_j) > 0 \\ 0 \text{ if } (x_i - x_j) = 0 \\ -1 \text{ if } (x_i - x_j) < 0 \end{cases} \tag{2}$$

The variance (σ^2) can be expressed as reported in Pohlert (2020):

$$\text{Var}(S) = \sigma^2 = \frac{\{n(n-1)(2n+5) - \sum_{j=1}^{p^*} t_j(t_j-1)(2t_j+5)\}}{18} \tag{3}$$

where p^* = number of the tied groups in the dataset and t_j = number of data points in *j*th tied group. The statistic *S* is distributed normally providing that *Z*-transformation is employed as given below:

$$Z = \begin{cases} \frac{S-1}{\sqrt{\text{var}(S)}} \text{ or } \frac{S-1}{\sigma}, \text{ if } S > 0 \\ 0 \text{ if } S = 0 \\ \frac{S+1}{\sqrt{\text{var}(S)}} \text{ or } \frac{S+1}{\sigma}, \text{ if } S < 0 \end{cases} \tag{4}$$

where $\sigma = SD = \sqrt{\frac{\{n(n-1)(2n+5) - \sum_{j=1}^{p^*} t_j(t_j-1)(2t_j+5)\}}{18}}$

The positive and negative *Z* values indicate increasing and decreasing trends, respectively. The critical values of *Z* are ± 1.96 at 5% level of significance. For $|Z| > 1.96$ at 5% level of significance, the null hypothesis can be rejected, and a trend can be recorded. In the present study, the hypothesis was tested at 5% level of significance (i.e., $\alpha = 0.05$).

Kendall’s tau (τ) is closely related to the statistic *S* as expressed in Pohlert (2020):

$$\tau = \frac{S}{\sqrt{\frac{n(n-1)}{2} \times \sqrt{\frac{n(n-1)}{2} - \frac{\sum_{j=1}^p t_j(t_j-1)}{2}}}} \tag{6}$$

Sens’s slope estimator

Mann–Kendal test has a limitation that it only confirms the existence of a significant trend if any for a given level of

significance. Thus, a non-parametric procedure developed by Theil (1950) and Sen (1968), known as Sen’s slope estimator (β), was used to calculate the magnitude of the trend (Eq. 7). Once the trend is detected in the time-series data, its magnitude or amplitude can also be determined by slope of the trend. The negative and positive β value indicates downward and upward trend, respectively. For a linear trend in the given time series data, β for n data pairs can be computed as

$$\beta = \text{Median} \left(\frac{x_i - x_j}{i - j} \right) \forall i < j (1 \leq i < j \leq n) \tag{7}$$

when n is even, median can be computed as

$$\text{Median} = \beta_{\frac{n+1}{2}} \tag{7a}$$

when n is odd, median can be computed as

$$\text{Median} = \frac{1}{2} (\beta_{\frac{n}{2}} + \beta_{\frac{n}{2}+1}) \tag{7b}$$

Change-point detection in time series data

Change-point detection in long-term time series data is important to examine the time period for a significant change. In the present case, standard normal homogeneity test (SNHT) and Pettitt’s test (Gallagher et al. 2012; Jaiswal and Lohani 2015) were applied using Monte Carlo method to check the homogeneity of data or to detect the change-point (Vezzoli et al. 2012), whether the time series data is homogeneous or not (when temporal changes or breaks are there). These two tests do not require any assumption related to the distribution of temperature (minimum and maximum), ET_o , and rainfall data. The test interpretation criteria were based on two hypotheses, viz., null hypothesis (H_0), i.e., data are homogeneous, and alternate hypothesis (H_a), i.e., there exists a date at which there is a change in data.

Standard normal homogeneity test (SNHT)

Standard normal homogeneity (SNHT), a non-parametric test developed by Alexandersson (1986), was further improved (Alexandersson and Moberg 1997) for detecting a change in a time series data. Test statistic (T_k) can be utilized to compare the mean of first n observations, with the remaining mean of $n - k$ observations having n number of data points (Stepanek et al. 2009; Vezzoli et al. 2012).

$$T_k = kZ_a^2 + (n - k)Z_b^2 \tag{8}$$

where,

$$Z_a = k^{-1} \sum_{i=1}^k \frac{x_i - \bar{x}}{\sigma_x} \tag{9}$$

$$Z_b = (n - k)^{-1} \sum_{i=k+1}^n \frac{x_i - \bar{x}}{\sigma_x} \tag{10}$$

where \bar{x} = mean, σ_x = standard deviation, and k = change point containing a break, at which the T_k value touches its maximum. For rejecting the H_0 , the critical value must be smaller than a test statistic, which is further dependent on number of observations (n). The p value is calculated using Monte Carlo simulations.

Pettitt’s test

Pettitt’s test was developed by Pettitt (1979) and can be advantageous in detecting any single change in hydrological or climate series with continuous data (Mu et al. 2007; Gao et al. 2011). It is also a non-parametric test and used without considering any assumption related to distribution of the time-series data. It is widely adopted for change-point detection in time series data, due to its sensitivity to changes or breaks (Winingaard et al. 2003). Different authors (Kang and Yusof 2012; Ilori and Ajayi 2020) have applied the test statistics used in Pettitt’s test. If t be the change point time in an observed data series of $x_1, x_2, x_3, \dots, x_n$, such that the first distribution function ($G_1(x)$) for the first part of the data series, i.e., $x_1, x_2, x_3, \dots, x_t$, is different from the second distribution function ($G_2(x)$) for the second part of the data series, i.e., $x_{t+1}, x_{t+2}, x_{t+3}, \dots, x_{t+n}$. According to this test, the variables either follow at least one distribution having no change for same location (H_0) or do not follow any distributions, having change in data series (H_a). The non-parametric function test statistics (U_t) is expressed as reported in Ilori and Ajayi (2020):

$$U_t = \sum_{i=1}^t \sum_{j=t+1}^n \text{sign}(x_i - x_j) \tag{11}$$

$$\text{sign}(x_i - x_j) = \begin{cases} 1 & \text{if } (x_i - x_j) > 0 \\ 0 & \text{if } (x_i - x_j) = 0 \\ -1 & \text{if } (x_i - x_j) < 0 \end{cases} \tag{12}$$

If the length of the sample and confidence interval be n and ρ , respectively, the test statistics K can be described as indicated by Eq. 13.

$$K = \text{Max} |U_t| \tag{13}$$

If the change-point of the time-series data is located at K providing that the statistic is significant, p value can be estimated as

$$p \cong 2 \times \exp\left(\frac{-6K^2}{n^2 + n^3}\right) \tag{14}$$

At change-point, the entire data series is separated into two sub-series. The probability at a change point (p_{cp}) can be defined by Eq. 15.

$$p_{cp} = 1 - p \tag{15}$$

Modeling of ET_o

Linear regression technique (in XLSTAT software) was used to formulate models for predicting ET_o on seasonal as well as annual basis in the present study region. The ET_o data for first 30 years (1970–1999) were utilized for developing the regression models, and the data from the next 20 years (2000–2019) were used for validating the developed models. The followings models were developed:

$$ET_o(\text{Spring}) = -0.35736 + 0.11549 \times T_{max} - 0.00884 \times T_{min} - 0.00849 \times RH_{max} - 0.01249 \times RH_{min} + 1.02396 \times v_w + 0.16160 \times SSH \tag{16}$$

$$ET_o(\text{Summer}) = -1.52235 + 0.13108 \times T_{max} + 0.03936 \times T_{min} - 0.01611 \times RH_{max} - 0.00643 \times RH_{min} + 0.64846 \times v_w + 0.25178 \times SSH \tag{17}$$

$$ET_o(\text{Autumn}) = -0.64190 + 0.06707 \times T_{max} + 0.01361 \times T_{min} - 0.00752 \times RH_{max} + 0.00303 \times RH_{min} + 0.94177 \times v_w + 0.15548 \times SSH \tag{18}$$

$$ET_o(\text{Winter}) = 1.37131 + 0.05079 \times T_{max} + 0.01057 \times T_{min} - 0.00575 \times RH_{max} - 0.01210 \times RH_{min} + 0.40747 \times v_w + 0.01372 \times SSH \tag{19}$$

$$ET_o(\text{Annual}) = -0.95870 + 0.08887 \times T_{max} + 0.02275 \times T_{min} - 0.00922 \times RH_{max} + 0.00039 \times RH_{min} + 0.87735 \times v_w + 0.18867 \times SSH \tag{20}$$

where T_{max} = maximum temperature ($^{\circ}\text{C}$), T_{min} = minimum temperature ($^{\circ}\text{C}$), RH_{max} = maximum relative humidity (%), RH_{min} = minimum relative humidity (%), v_w = wind speed (m/s), and SSH = sunshine hours.

Statistical analysis

The statistical analysis involved computation of mean, median, standard deviation (σ), variance (σ^2), mean bias error (MBE), mean absolute error (MAE), root mean square

error (RMSE), and Willmott index of agreement (d). MAE, RMSE, coefficient of determination (r^2), σ , and d values were used in testing the performance of developed ET_o models.

Mean bias error (MBE)

$$MBE = \frac{1}{n} \sum_{i=1}^n (P_i - O_i) \tag{21}$$

Mean absolute error (MAE)

$$MAE = \frac{1}{n} \sum_{i=1}^n |P_i - O_i| \tag{22}$$

Root mean square error (RMSE)

$$RMSE = \sqrt{\frac{1}{n} \sum_{i=1}^n (P_i - O_i)^2} \tag{23}$$

Standard deviation (SD)

$$SD = \sqrt{RMSE^2 - MBE^2} \tag{24}$$

Index of agreement (d)

$$d = 1 - \left(\frac{\sum_{i=1}^n (P_i - O_i)^2}{\sum_{i=1}^n (|P_i - \bar{O}| + |O_i - \bar{O}|)^2} \right)^{1/2}, [0 \leq d \leq 1] \tag{25}$$

where n = number of data points, P_i = predicted or estimated data, and O_i = observed or standard data.

Results and discussion

Mann–Kendall's trend analysis

The long-term minimum temperature (T_{min}) was recorded to be in the range of 15.0–19.8 $^{\circ}\text{C}$, 23.3–27.5 $^{\circ}\text{C}$, 14.1–18.8 $^{\circ}\text{C}$, and 4.5–8.5 $^{\circ}\text{C}$ for spring, summer, autumn, and winter seasons, respectively, whereas on annual basis, it was recorded as 14.8–18.5 $^{\circ}\text{C}$. For T_{min} , the Kendall's tau (τ) value was recorded to be positive for all the four seasons, as well as on annual basis and varied from 0.468 (winter) to 0.531 (summer), being 0.631 on annual basis (Table 1). There existed a

significant trend (increasing) in long-term T_{\min} data during all the four seasons (spring, summer, autumn, and winter), as well as on annual basis ($p < 0.05$ (α) in each case) for 5% level of significance. Earlier, Grover and Upadhaya (2014) have reported a significant increase (1.4–2.1 °C) in T_{\min} during kharif season in the present study region. Kaur et al. (2016) have also reported an increasing trend in T_{\min} from year 1970 to 1990. Further, Kingra (2018) has confirmed the increasing trend in long-term T_{\min} in the same region for a period from 1970 to 2014. However, this increasing trend in T_{\min} with time, particularly during the months of February and March, may significantly reduce the yield of wheat crop grown in the region as these two months correspond to grain filling in wheat crop (Kaur et al. 2012). The long-term maximum temperature (T_{\max}) was recorded to be in the range of 29.5–36.6 °C, 33.6–37.3 °C, 28.7–31.9 °C, and 18.2–22.0 °C during spring, summer, autumn, and winter seasons, respectively, with the annual T_{\max} as 28.2–30.7 °C, being lowest and highest during winter and summer seasons, respectively. For T_{\max} , the τ value was recorded to be positive for spring and on annual basis, whereas negative for rest of the three seasons (summer, autumn, and winter). The τ value was recorded to be 0.111, –0.078, –0.145, –0.117, and 0.010 for spring, summer, autumn, winter, and annual basis, respectively. No definite trend was recorded in the long-term data of T_{\max} for all the four respective seasons, as well as on annual basis (Table 1). Similar observation related to trend in long-term T_{\max} has been reported by Kingra (2018). The average temperature (T_{\min} and T_{\max}) was recorded to be highest during summer followed by spring, autumn, and winter (least).

The rainfall during spring, summer, autumn, and winter seasons was recorded to be in the range of 9.7–191.7 mm, 97.6–822.8 mm, 6.7–668.6 mm, and 2.0–202.5 mm, respectively, whereas on annual basis, it varied as 379.6–1334 mm with average value of 747.4 mm. The average seasonal rainfall during study period was recorded to be highest during summer (485.9 mm) followed by autumn (123.3 mm) and least during spring (63.7 mm). The τ values for rainfall were recorded to be positive for all seasons, except during summer (negative). The τ value was recorded to be 0.071, –0.019, 0.138, 0.043, and 0.031 for spring, summer, autumn, winter, and annual basis, respectively. No trend (insignificant) was recorded in the long-term rainfall data for all the four respective seasons, as well as on annual basis (Table 1). Similar observation related to rainfall has been made by Kashyap and Agarwal (2020). A significant trend (decreasing) was recorded in long-term ET_o during all the four seasons (spring, summer, autumn, and winter), as well as on annual basis ($p < 0.05$ (α) in each case) for 5% level of significance. Similar observation related to ET_o has been reported in Kashyap and Agarwal (2020). ET_o was estimated to be in the range of 4.69–6.01 mm/day, 4.70–6.43 mm/day,

2.74–3.66 mm/day, and 1.49–2.27 mm/day during spring, summer, autumn, and winter seasons, respectively, whereas it varied in the range of 3.57–4.39 mm/day on annual basis, being lowest and highest during winter and spring seasons, respectively. Similar range of annual ET_o (3.52–4.27 mm/day) has been reported by Kingra (2018) for the same region for a study period from 1970 to 2014. Thus, decreasing ET_o , particularly in relation to increasing T_{\min} , confirms the presence of an evaporation paradox in the study area. The declining ET_o may result in decreased crop water requirements. Kashyap and Agarwal (2020) have reported increasing trend in crop yields (rice and wheat) for the present study region with decrease in ET_o . In case of ET_o , the value of τ was computed to be negative for all the four seasons as well as on annual basis. The τ value varied from –0.663 (for autumn) to –0.313 (for spring), whereas it was computed to be –0.609 on annual basis. The average ET_o was recorded to be highest during spring (5.44 mm/day) followed by summer (5.44 mm/day), autumn (3.66 mm/day), and winter (1.79 mm/day). On annual basis, the average ET_o was computed as 3.98 mm/day. The estimated ET_o was obtained in the order as follows: ET_o (spring) \geq ET_o (summer) $>$ ET_o (autumn) $>$ ET_o (winter). Irrespective of the higher temperature during summer as compared to spring, the ET_o during summer was slightly lower as compared to spring.

Sen's slope trend analysis

From the results of Sen's slope test, an upward (increasing) trend was recorded in T_{\min} data during all the four respective seasons as well as on annual basis. Similar trend in T_{\min} has been reported by Kaur et al. (2012) and Grover and Upadhaya (2014) for the same region. The Sen's slope varied from 0.042 to 0.060, having lowest and highest values during summer and spring seasons, respectively (Table 2). On annual basis, the Sen's slope was recorded as 0.050. The increasing trend in T_{\min} in the present study region (from 1970 to 2006) on annual basis has also been reported in Kaur et al. (2006). Further, similar trend in T_{\min} has been reported in Kaur et al. (2016). In case of T_{\max} , an upward (increasing) trend was recorded during spring season (Sen's slope = 0.017) as well as on annual basis (Sen's slope = 0.001) as also reported in Kaur et al. (2016), whereas during summer, autumn, and winter seasons, a downward trend was recorded. Thus, the trend in T_{\max} was mainly downward or decreasing (from 1970 to 2006) as reported by Kaur et al. (2006), except during spring season and on annual basis. Similar observation has also been made by Kaur et al. (2012). The Sen's slope varied from –0.010 to 0.017 (Table 2), having lowest and highest values during winter and spring seasons, respectively. On annual basis, the Sen's slope was recorded as 0.001. In case of rainfall, an upward (increasing) trend was recorded during spring,

Table 1 Parameters of Mann–Kendall’s trend analysis test

Parameter	Season	Range	Mean	SD	τ	S	Var (S)	p value	α	Test interpretation
ET ₀ (mm/season or mm/year)	Spring	4.69–6.01	5.44	0.27	-0.3129	-368	0.0000	0.0013	0.05	There is a trend in the series (p value < α)
	Summer	4.70–6.43	5.44	0.40	-0.3197	-376	0.0000	0.0010	0.05	There is a trend in the series (p value < α)
T _{min} (°C)	Autumn	2.74–3.66	3.23	0.23	-0.6633	-780	0.0000	<0.0001	0.05	There is a trend in the series (p value < α)
	Winter	1.49–2.27	1.79	0.17	-0.5782	-680	0.0000	<0.0001	0.05	There is a trend in the series (p value < α)
	Annual	3.57–4.39	3.97	0.20	-0.6088	-716	0.0000	<0.0001	0.05	There is a trend in the series (p value < α)
	Spring	15.0–19.8	17.35	1.15	0.514	604	13,458.7	<0.0001	0.05	There is a trend in the series (p value < α)
	Summer	23.3–27.5	25.92	0.86	0.531	624	13,458.7	<0.0001	0.05	There is a trend in the series (p value < α)
	Autumn	14.1–18.8	16.79	1.1	0.476	560	13,458.7	<0.0001	0.05	There is a trend in the series (p value < α)
	Winter	4.5–8.5	6.72	1.01	0.468	550	13,458.7	<0.0001	0.05	There is a trend in the series (p value < α)
	Annual	14.8–18.5	16.69	0.88	0.631	742	13,458.7	<0.0001	0.05	There is a trend in the series (p value < α)
	Spring	29.5–36.6	33.35	1.39	0.111	130	13,458.7	0.266	0.05	There is no trend in the series (p value > α)
	Summer	33.6–37.3	35.21	0.81	-0.078	-92	13,458.7	0.433	0.05	There is no trend in the series (p value > α)
	Autumn	28.7–31.9	30.59	0.59	-0.145	-170	13,458.7	0.145	0.05	There is no trend in the series (p value > α)
	Winter	18.2–22.0	19.94	0.84	-0.117	-138	13,458.7	0.238	0.05	There is no trend in the series (p value > α)
Rainfall (mm)	Annual	28.2–30.7	29.78	0.53	0.01	12	13,458.7	0.924	0.05	There is no trend in the series (p value > α)
	Spring	9.2–191.7	63.66	43.94	0.071	84	13,458.7	0.474	0.05	There is no trend in the series (p value > α)
	Summer	97.6–822.8	485.88	162.34	-0.019	-22	13,458.7	0.856	0.05	There is no trend in the series (p value > α)
	Autumn	6.7–668.6	123.33	126.55	0.138	162	13,458.7	0.165	0.05	There is no trend in the series (p value > α)
	Winter	2.0–202.5	76.81	47.61	0.043	50	13,456.7	0.673	0.05	There is no trend in the series (p value > α)
	Annual	379.6–1334.0	747.35	222.24	0.031	37	13,457.7	0.756	0.05	There is no trend in the series (p value > α)

autumn, winter, and on annual basis, whereas a downward (decreasing) trend during summer season. Kaur et al. (2016) have also reported an increasing trend in rainfall in the region from year 1970 to 1990. Further, Krishan et al. (2015) have reported an increasing trend in annual rainfall in this region (from year 1901 to 2002). Similar trend in long-term rainfall of the present study region (1970 to 2006) has been reported by Kaur et al. (2006). The Sen’s slope varied from -0.297 to 0.830 (Table 2), having lowest and highest values during summer and autumn seasons, respectively. On annual basis, the Sen’s slope was recorded as 0.663 . The estimated ET_o data indicated a downward (decreasing) trend during all the four respective seasons as well as on annual basis. The Sen’s slope varied from -0.0139 to -0.0084 , having lowest and highest values during autumn and spring seasons, respectively (Table 2). On annual basis, the Sen’s slope was recorded as -0.0104 . The Sen’s slope test indicated a downward trend in ET_o with increase in T_{min} during all the four respective seasons as well as on annual basis. Overall, the Sen’s slope analysis indicated increasing (upward) and decreasing (downward) trend in long-term T_{min} and ET_o , respectively, with time. ET_o may also decrease with decrease in T_{max} (during summer, autumn, and winter) and rainfall

(during summer season). Unlike T_{min} and ET_o , the trend in T_{max} and rainfall were recorded to be either increasing or decreasing, indicating no definite trend throughout the year. Similarly, Kaur et al. (2012) have reported no definite trend in T_{max} , unlike T_{min} . The Sen’s slope test confirms the results of Mann–Kendall’s test for T_{min} and ET_o .

Homogeneity test for change-point detection in T_{min} , T_{max} , ET_o , and rainfall data

In standard normal homogeneity test (SNHT) and Pettitt’s test, using Monte Carlo simulations (10,000) was applied at 99% confidence interval on the p value (two-tailed test). As per both SNHT and Pettitt’s tests, change-points were detected in both T_{min} and ET_o data during all four seasons, as well as on annual basis. The p value was recorded to be lower than α value (0.05) indicating existence of a date at which there is a change in T_{min} and ET_o data (Table 3), both seasonally and annually. Jaiswal et al. (2015) and Ilori and Ajay (2020) have also reported change points in long-term T_{min} and T_{mean} , respectively, indicating the increasing trend with time. The mean T_{min} values before and after change-point during spring, summer, autumn, winter, and on annual basis were recorded as 16.6 °C and 18.3 °C, 25.0 °C and 26.3 °C, 15.6 °C and 17.3 °C, 5.8 °C and 7.2 °C, and 15.7 °C and 17.1 °C, respectively (Fig. 2a–e). Figure 2 demonstrates the presence of change-point and trend in T_{min} during four respective seasons as well as on annual basis. In case of T_{max} , a change-point was detected only during spring season (Fig. 3a), having the mean T_{max} values before and after change-point as 32.9 °C and 34.1 °C, respectively (Fig. 3a). Whereas during summer, autumn, winter, and on annual basis, the mean T_{max} value was recorded as 35.2 , 30.6 , 19.9 , and 29.8 °C, respectively (Fig. 3b–e), indicating homogeneity (absence of change-point) in data series. The rainfall data was observed to be homogeneous. The rainfall was recorded as 63.7 , 485.9 , 123.3 , 76.8 , and 747.4 mm during spring, summer, autumn, winter, and on annual basis, respectively (Fig. 4a–e). Figure 4 demonstrates the absence of change-point and trend in rainfall during four respective seasons as well as on annual basis. The rainfall and T_{max} were observed to be homogeneous (i.e., no change-point). The parameters of change-point detection in time-series data are presented in Table 3. The mean ET_o values before and after change-point during spring, summer, autumn, winter, and on annual basis were recorded as 5.68 mm/day and 5.36 mm/day, 5.66 mm/day and 5.23 mm/day, 3.39 mm/day and 3.03 mm/day, 1.89 mm/day and 1.66 mm/day, and 4.12 mm/day and 3.84 mm/day, respectively (Fig. 5a–e), indicating decline in ET_o after the change-points. Figure 5 demonstrates the presence of change-point and trend in ET_o during four respective seasons as well as on annual basis.

Table 2 Sen’s slope values during different seasons as well as on annual basis

Parameter	Season	Sen’s slope		
		Sen’s slope	Confidence interval	
			Lower bound (95%)	Upper bound (95%)
ET_o	Spring	-0.0084	-0.0970	0.0712
	Summer	-0.0119	-0.1396	0.1313
	Autumn	-0.0139	-0.0514	0.0321
	Winter	-0.0091	-0.0499	0.0365
	Annual	-0.0104	-0.0561	0.0358
T_{min}	Spring	0.06	0.04	0.079
	Summer	0.042	0.03	0.054
	Autumn	0.053	0.035	0.071
	Winter	0.049	0.03	0.064
	Annual	0.05	0.039	0.061
T_{max}	Spring	0.017	-0.012	0.05
	Summer	-0.007	-0.024	0.009
	Autumn	-0.006	-0.015	0.003
	Winter	-0.01	-0.027	0.008
	Annual	0.001	-0.011	0.011
Rainfall (mm)	Spring	0.327	-0.535	0.933
	Summer	-0.297	-3.682	3.024
	Autumn	0.830	-0.469	2.341
	Winter	0.252	-0.750	1.115
	Annual	0.663	-3.710	4.818

Table 3 Parameters of homogeneity analysis

Parameter	Season	Standard normal homogeneity test (SNHT)				Pettitt's test		
		T_0 or K	t	p value*	K	t	p value*	α
T_{\min}	Spring	24.72	1997	<0.0001	506	1997	<0.0001	0.05
	Summer	24.57	1983	<0.0001	482	1989	<0.0001	0.05
	Autumn	24.25	1984	<0.0001	450	1996	<0.0001	0.05
	Winter	21.47	1985	<0.0001	448	1988	<0.0001	0.05
	Annual	28.56	1984	<0.0001	542	1997	<0.0001	0.05
T_{\max}	Spring	8.87	1998	0.036	278	1997	0.024	0.05
	Summer	4.68	1987	0.33	188	1987	0.252	0.05
	Autumn	3.65	1974	0.554	210	1983	0.15	0.05
	Winter	2.67	1970	0.738	140	1987	0.583	0.05
	Annual	3.25	1998	0.574	174	1998	0.331	0.05
ET_0	Spring	13.21	1981	0.0036	344	1981	0.0021	0.05
	Summer	13.91	1993	0.0028	356	1993	0.0006	0.05
	Autumn	30.21	1996	<0.0001	562	1996	<0.0001	0.05
	Winter	23.37	1996	<0.0001	516	1996	<0.0001	0.05
	Annual	24.98	1993	<0.0001	528	1993	<0.0001	0.05
Rainfall	Spring	4.12	1976	0.421	158.00	1976	0.429	0.05
	Summer	0.73	2011	1.000	86.00	2001	0.961	0.05
	Autumn	4.17	1987	0.406	196.00	1983	0.202	0.05
	Winter	3.24	2017	0.612	79.00	2011	0.984	0.05
	Annual	1.82	1974	0.907	98.00	1982	0.915	0.05

* p value (two-tailed) was computed using 10,000 Monte Carlo simulations (time elapsed: 0 s) (99% confidence interval on the p value)

The SNHT recorded 1997, 1983, 1984, 1985, and 1984 as change-point years in T_{\min} during spring, summer, autumn, winter, and on annual basis, respectively, whereas the Pettitt's test recorded the change-points in years 1997, 1989, 1996, 1988, and 1997, during four respective seasons and on annual basis. For spring season, the change-point (year 1997) in T_{\min} was recorded to be same as per both tests. For T_{\max} , both tests (SNHT and Pettitt's) recorded change-points in 1998 and 1997, respectively, for spring season only. Separately, in T_{\min} and T_{\max} , the change-points were recorded to be different by both tests, except in one season (spring) for T_{\min} . However, for ET_0 which is jointly affected by T_{\min} and T_{\max} , the change-points during all the four seasons as well as on annual basis were recorded to be same. The change-points recorded by both tests were 1981, 1993, 1996, 1996, and 1993, for spring, summer, autumn, winter, and on annual basis, respectively. ET_0 performed as a better representative of climate change in relation to temperature variation (T_{\min} and T_{\max}).

The seasonal lowest T_{\min} value was recorded to be in the range of 4.5–23.3 °C (being lowest and highest for winter and summer seasons, respectively), with an average value of 14.8 °C. Similarly, the seasonal highest T_{\min} value was recorded to be in the range of 8.5–27.5 °C (being lowest and highest for winter and summer seasons, respectively), with an average value of 18.5 °C (Fig. 6a–e). Figure 6

demonstrates the different statistical parameters estimated for all the seasons as well as on annual basis. The first quartile (Q_1) value for seasonal T_{\min} was recorded to be in the range of 6.0–25.5 °C, with an average value of 16.1 °C. Similarly, the third quartile (Q_3) for seasonal T_{\min} was recorded to be in the range of 7.3–26.5 °C, with an average value of 17.3 °C. The median value for seasonal T_{\min} was recorded to be in the range of 6.9–26.1 °C, with an average value of 16.8 °C. Similarly, the mean seasonal T_{\min} was computed in the range of 6.7–26.0 °C, with a mean value of 16.7 °C. The trend in T_{\min} , T_{\max} , Q_1 , Q_3 , median, and mean was similar (being lowest and highest for winter and spring seasons, respectively, in each case). However, the trend was slightly different for variance (σ_{n-1}^2) and standard deviation (σ_{n-1}) values. σ_{n-1}^2 value varied from 1.0 to 1.3 (lowest and highest values for winter and spring seasons, respectively), with an average value of 0.8 (Fig. 6a–e). Similarly, σ_{n-1} value varied from 1.0 to 1.2 °C (lowest and highest values for winter and spring seasons, respectively), with an average value of 0.9 °C.

The seasonal lowest T_{\max} value was computed to be in the range of 18.2–33.6 °C (being lowest and highest values for winter and summer seasons, respectively), with an average value of 28.2 °C (Fig. 7a–e). Figure 7 demonstrates the different statistical parameters estimated for all the seasons as well as on annual basis. Similarly, the seasonal highest

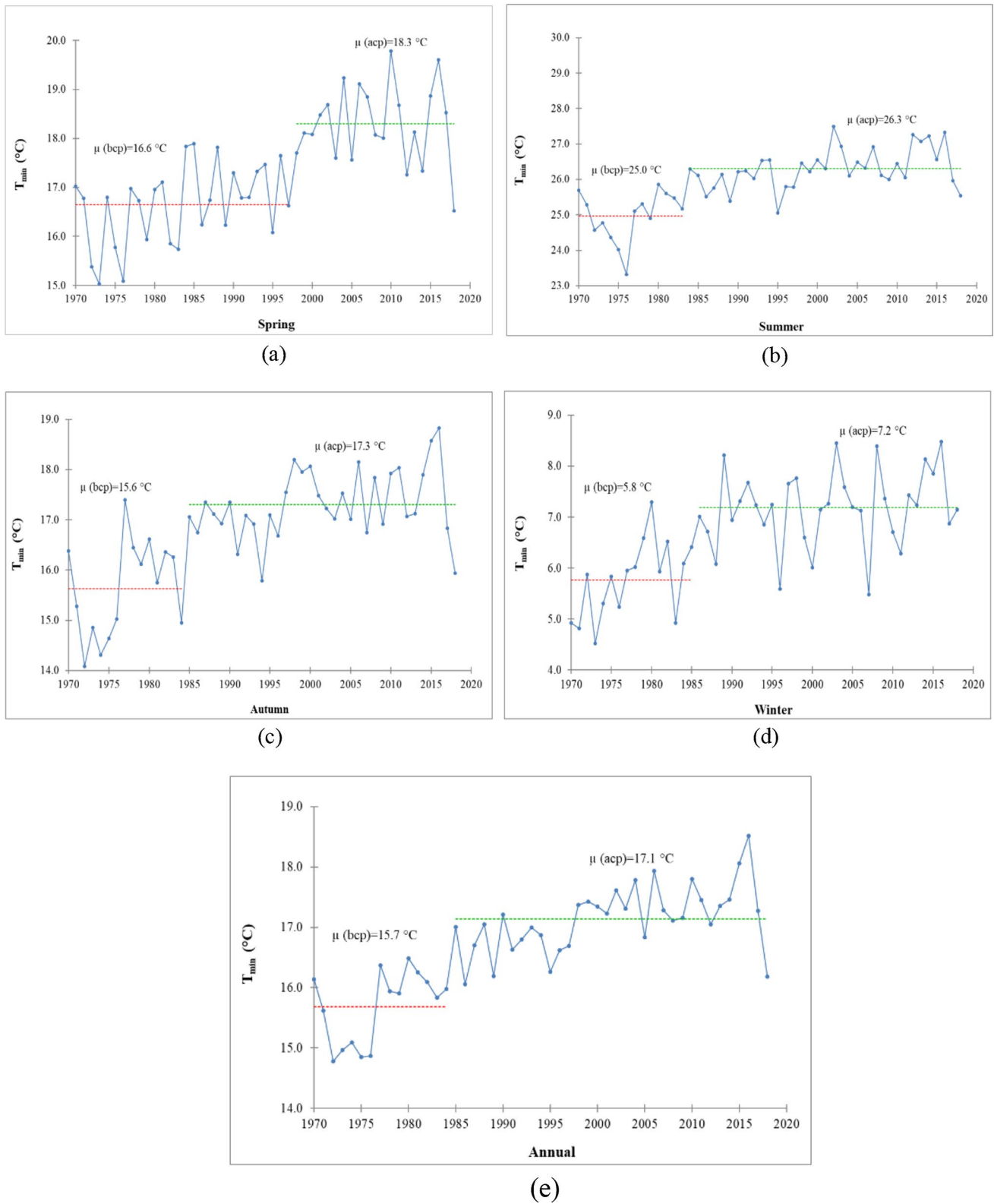


Fig. 2 Change-point detection in T_{min} during (a) spring, (b) summer, (c) autumn, (d) winter, and (e) on annual basis

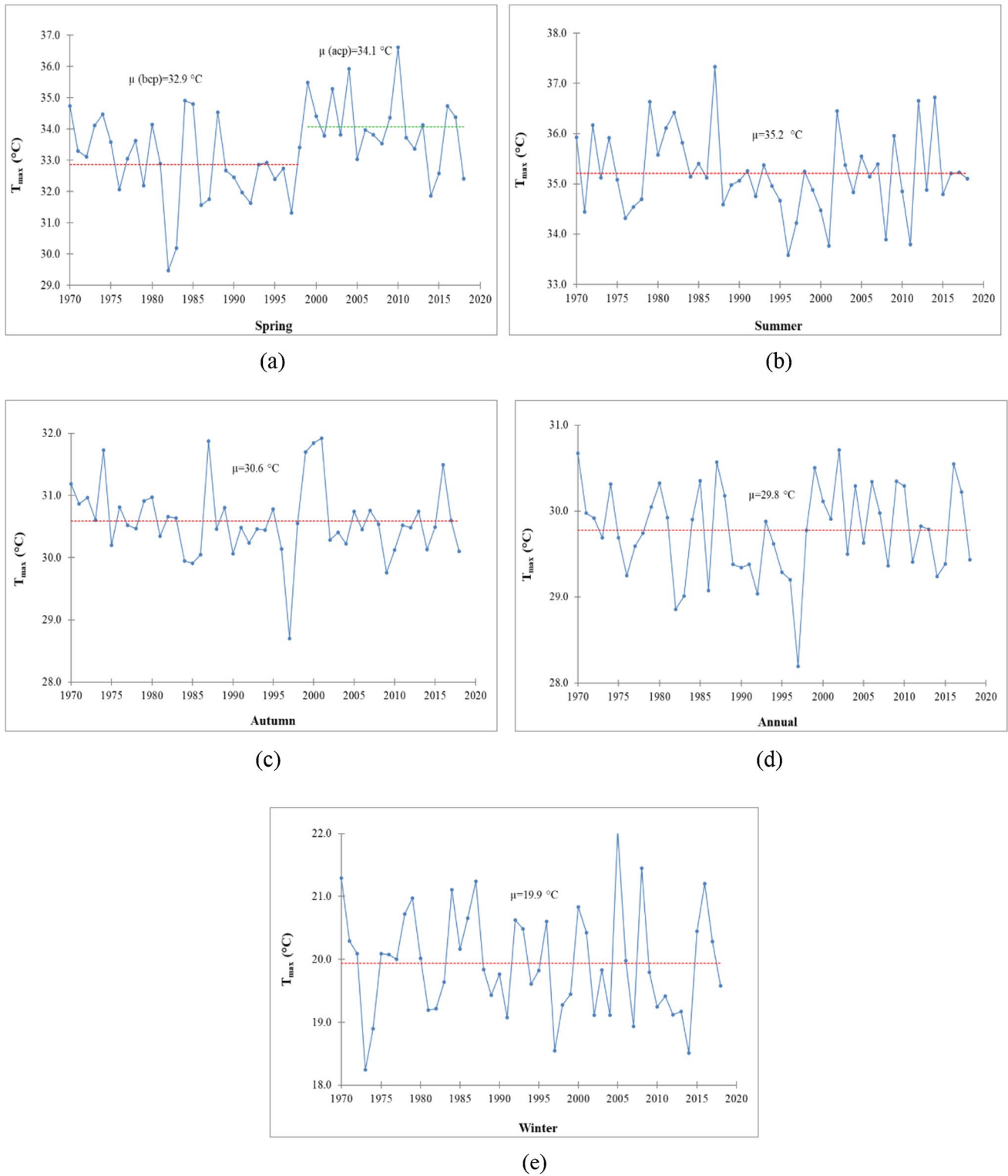


Fig. 3 Change-point detection in T_{max} during (a) spring, (b) summer, (c) autumn, (d) winter, and (e) on annual basis

T_{max} value was computed to be in the range of 22.0–37.3 °C (being lowest and highest values for winter and summer seasons, respectively), with an average value of 30.7 °C

(Fig. 7a–e). The Q_1 value was recorded to be in the range of 19.2–34.8 °C, with an average value of 29.4 °C. Similarly, Q_3 for seasonal T_{max} was recorded to be in the range

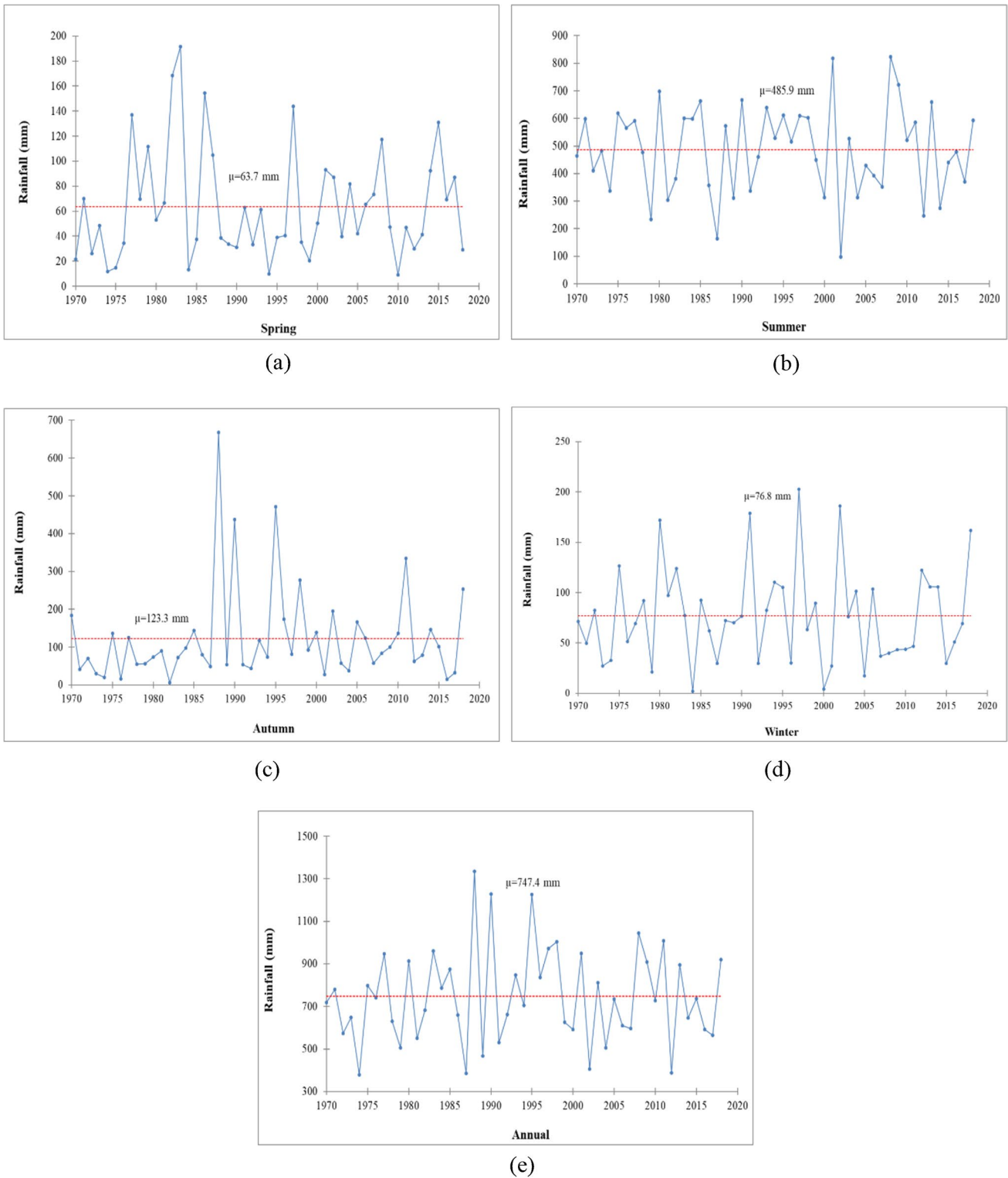


Fig. 4 Change-point detection in rainfall during (a) spring, (b) summer, (c) autumn, (d) winter, and (e) on annual basis

of 20.5–35.6 °C, with an average value of 30.2 °C on annual basis. The median value for seasonal T_{max} was recorded to be in the range of 19.8–35.1 °C, with an average value of

29.8 °C. Similarly, the mean seasonal T_{max} was computed in the range of 19.9–35.2 °C, with a mean value of 29.8 °C. As reported above, the trend in T_{min} , T_{max} , Q_1 , Q_3 , median

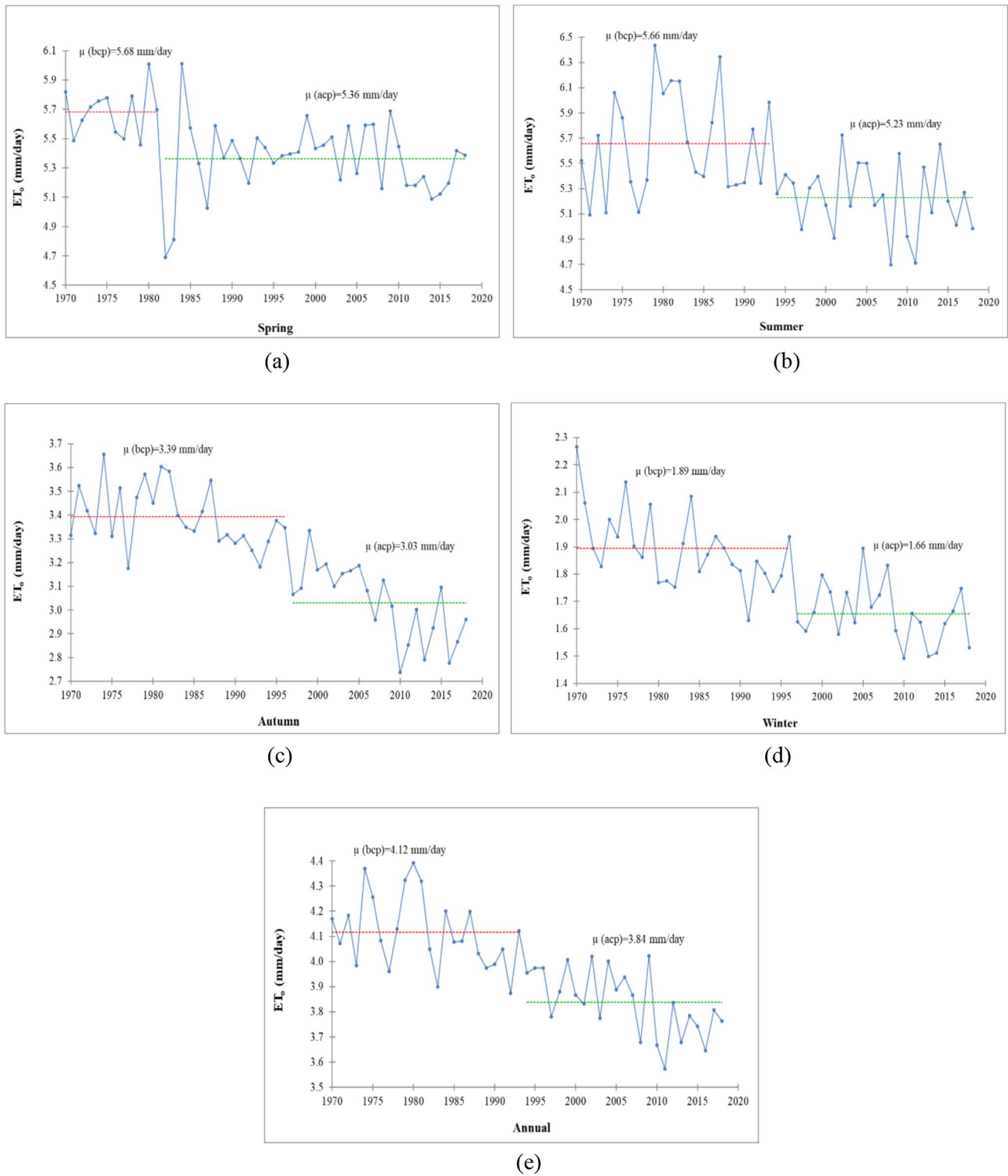
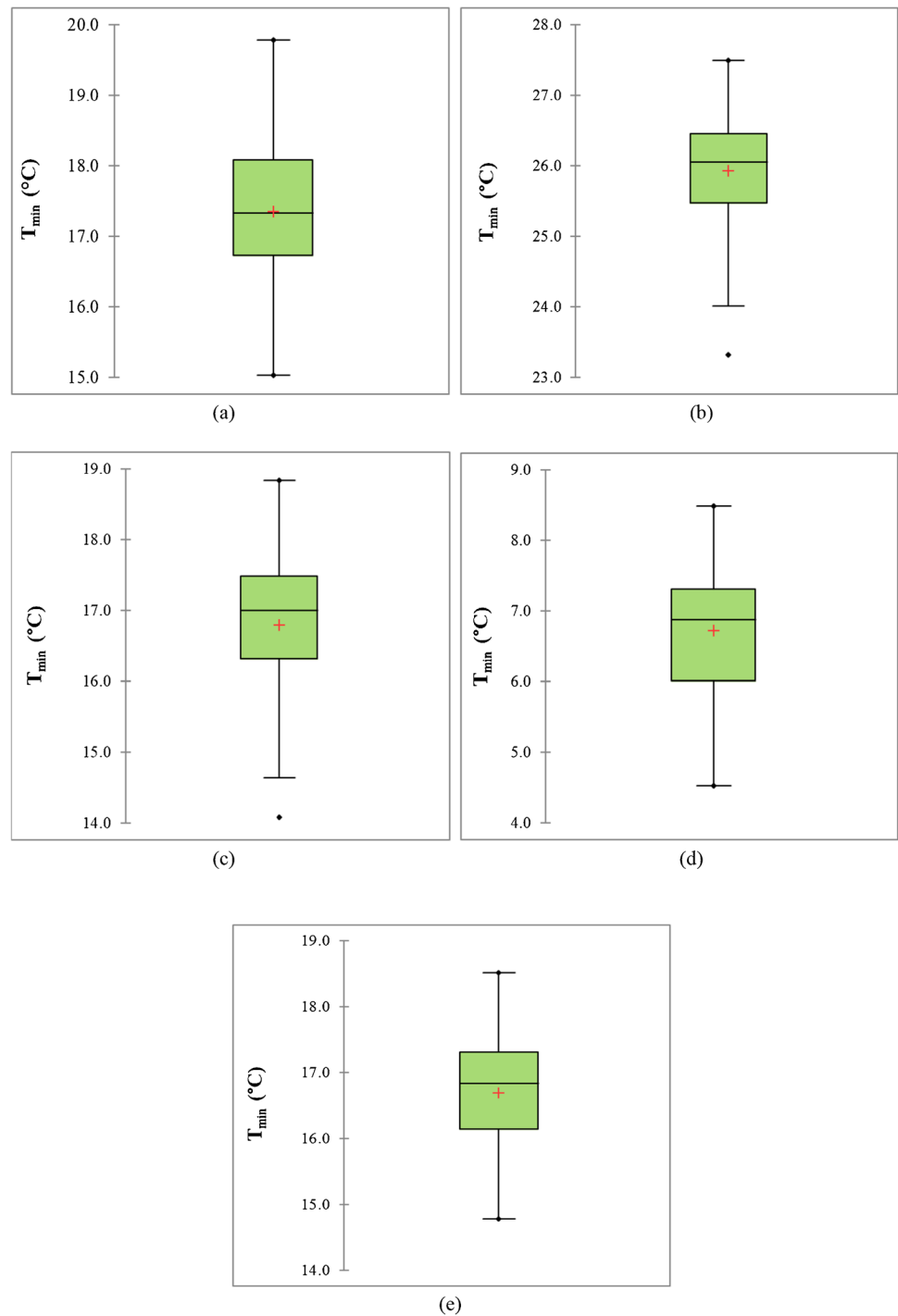


Fig. 5 Change-point detection in ET_0 during (a) spring, (b) summer, (c) autumn, (d) winter, and (e) on annual basis

and mean was similar (being lowest and highest for winter and spring seasons, respectively, in each case). However, the trend was slightly different for σ_{n-1}^2 and σ_{n-1} values. σ_{n-1}^2

value varied from 0.7 to 1.9 (lowest and highest values for winter and spring seasons, respectively), with an average value of 0.3 (Fig. 7a–e). Similarly, σ_{n-1} value varied from 0.8

Fig. 6 Depiction of parameters of statistical analysis for T_{min} during (a) spring, (b) summer, (c) autumn, (d) winter, and (e) on annual basis

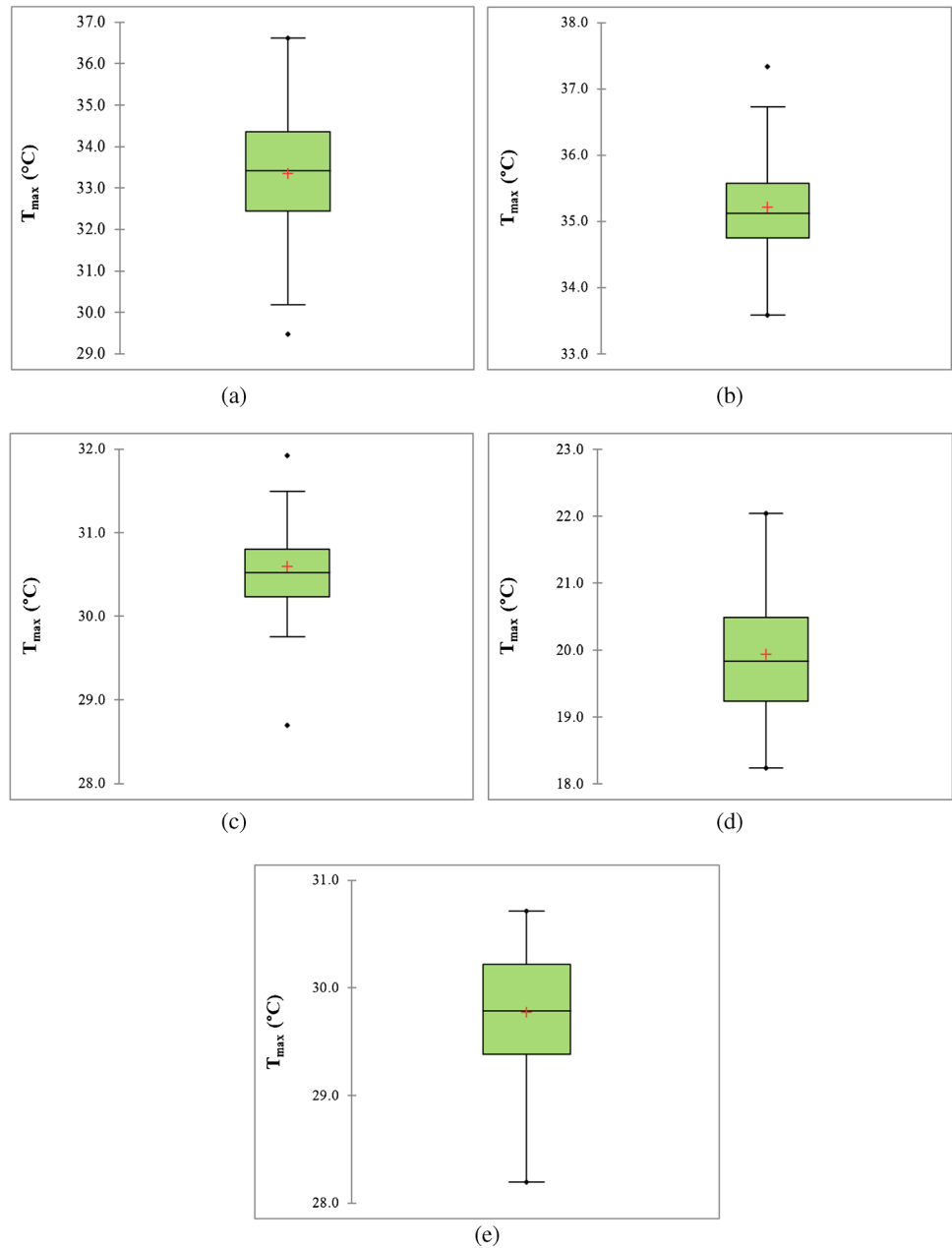


to 1.4 °C (lowest and highest values for winter and spring seasons, respectively), with an average value of 0.5 °C annual basis.

The seasonal lowest rainfall was recorded to be in the range of 2.0–97.6 mm (being lowest and highest values for winter and summer seasons, respectively), with a total of 379.6 mm. Similarly, the seasonal highest rainfall was recorded to be in the range of 191.7–822.8 mm, with a

total of 1334.0 mm (Fig. 8a–e), being minimum and maximum during spring and summer seasons, respectively. Figure 8 demonstrates the different statistical parameters estimated for all the seasons as well as on annual basis. The Q_1 value for seasonal rainfall was recorded to be in the range of 33.9–358.3 mm (having lowest and highest values for spring and summer seasons, respectively), with a total of 591.6 mm. Similarly, Q_3 was computed to be

Fig. 7 Depiction of parameters of statistical analysis for T_{max} during (a) spring, (b) summer, (c) autumn, (d) winter, and (e) on annual basis

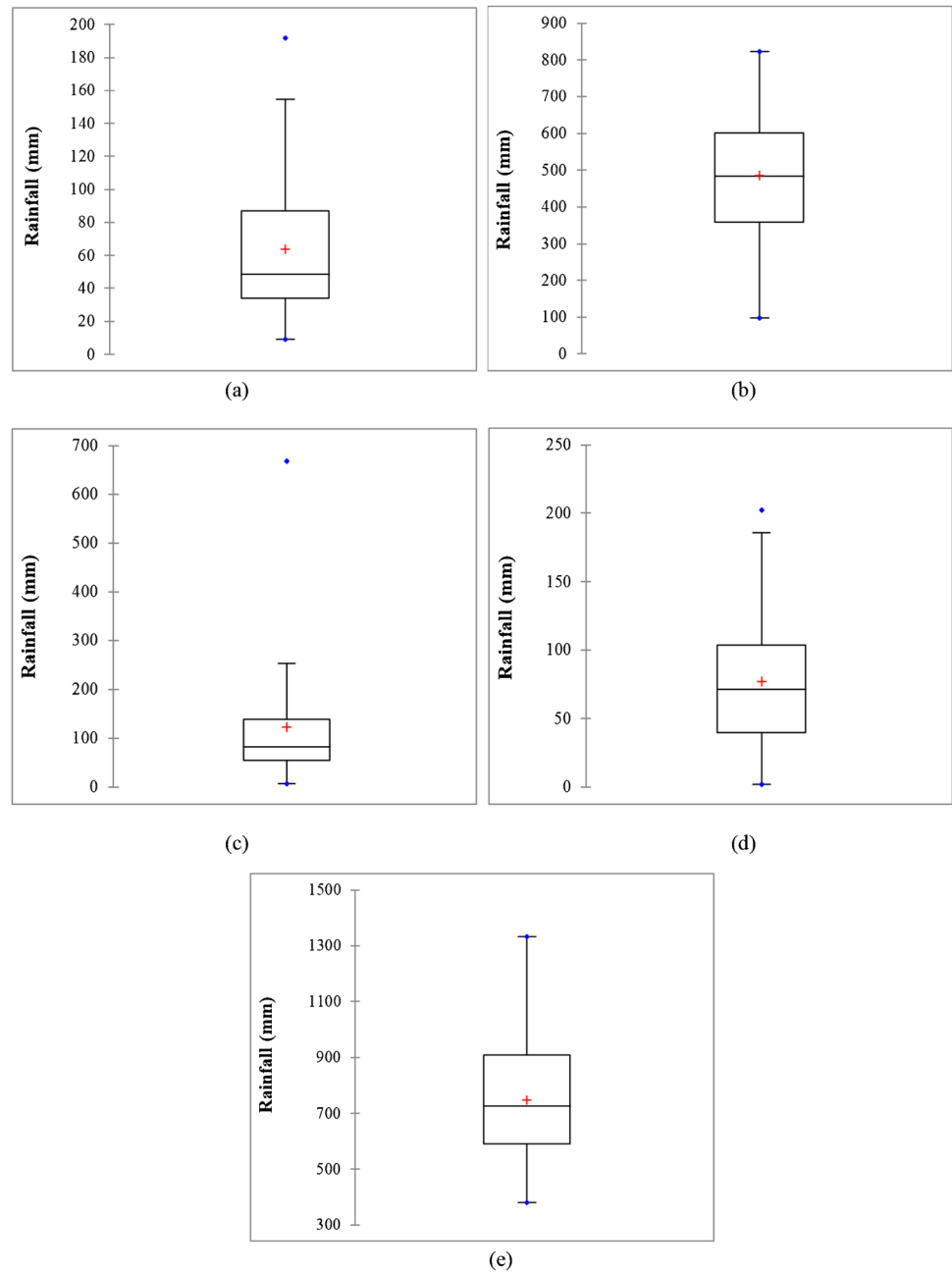


in the range of 87.2–600.6 mm (having lowest and highest values for spring and summer seasons, respectively), with a total of 909.2 mm. The median value for seasonal rainfall was recorded to be in the range of 48.4–483.1 mm (having lowest and highest values for spring and summer seasons, respectively), having a total of 727.0 mm. Similarly, the mean rainfall was recorded in the range of 63.7–485.9 mm (having lowest and highest values for spring and summer seasons, respectively), having a total of 747.4 mm. σ_n^2 varied from 1891.6 to 25,815.2 (lowest and highest values for spring and summer seasons, respectively), having a total of 48,383.6 (Fig. 8a–e). Similarly, σ_n and σ_{n-1} values varied from 43.5 to 160.7

(lowest and highest values for spring and summer seasons, respectively), having a total of 220.0.

The seasonal lowest ET_0 was computed to be in the range of 1.49–4.70 mm/day (being lowest and highest values for winter and summer seasons, respectively), with an average value of 5.44 mm/day. On annual basis, ET_0 was computed as 3.57 mm/day. Similarly, the seasonal highest ET_0 value was computed to be in the range of 2.27–6.43 mm/day (being lowest and highest values for winter and summer seasons, respectively), with an average value of 5.44 mm/day. The annual ET_0 was computed as 4.39 mm/day (Fig. 9a–e). Figure 9 demonstrates the different statistical parameters estimated

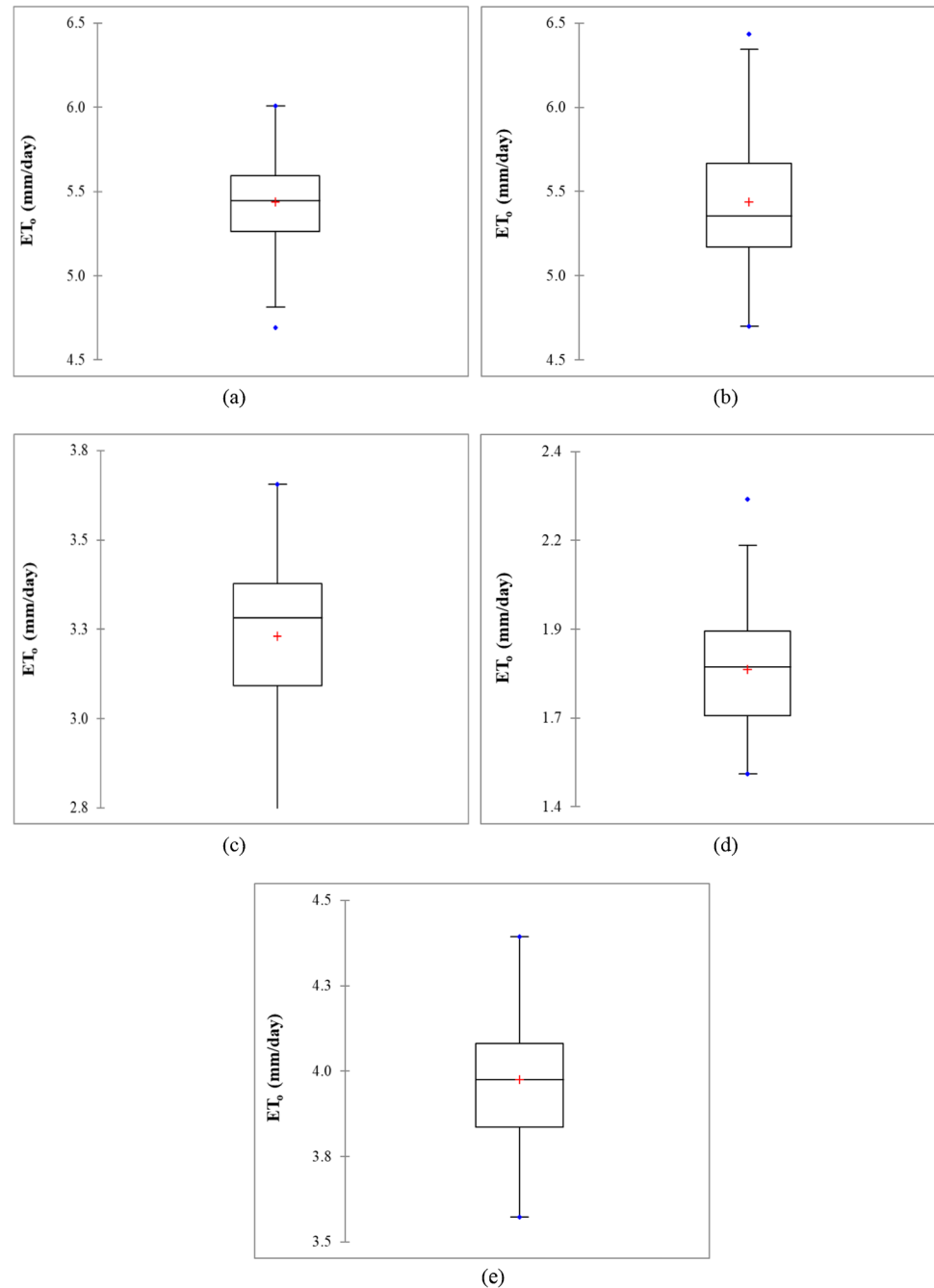
Fig. 8 Depiction of parameters of statistical analysis for rainfall during (a) spring, (b) summer, (c) autumn, (d) winter, and (e) on annual basis



for all the seasons as well as on annual basis. The Q_1 value for seasonal ET_0 was recorded to be in the range of 1.66–5.26 mm/day (having lowest and highest values for winter and spring seasons, respectively), with an average value of 3.84 mm/day. Similarly, Q_3 for seasonal ET_0 was recorded to be in the range of 1.89–5.67 mm/day (having lowest and highest values for winter and summer seasons, respectively), with an average value of 4.08 mm/day. The median value for seasonal ET_0 was recorded to be in the range of 1.79–5.45 mm/day (having lowest and highest values for winter and spring seasons,

respectively), with an average value of 3.98 mm/day. Similarly, the mean value for seasonal ET_0 was computed in the range of 1.79–5.44 mm/day (having lowest and highest values for winter and summer seasons, respectively), with an average value of 3.97 mm/day. σ_n^2 values varied from 0.03 to 0.16 (lowest and highest values for winter and summer seasons, respectively), with an average value of 0.04 (Fig. 9a–e). Similarly, σ_n values varied from 0.17 to 0.40 (lowest and highest values for winter and summer seasons, respectively), with an average value of 0.19.

Fig. 9 Depiction of parameters of statistical analysis for ET_o during (a) spring, (b) summer, (c) autumn, (d) winter, and (e) on annual basis



Inter-correlation test among estimated ET_o and recorded micro-meteorological parameters

For obtaining the inter-correlation between ET_o , T_{max} , T_{min} , RH_{max} , RH_{min} , v_w , SSH , and rainfall, a correlation matrices were obtained for all the four seasons as well as on annual basis using XLSTAT Software (Tables 4, 5, 6, 7 and 8). The absolute correlation coefficient values of >0.9 , >0.75 (>0.75 and ≤ 0.90), and >0.6 (>0.6 and ≤ 0.75) were used as standards for indicating strong, good, and moderate correlation, respectively, as suggested in Meshram and Sharma

(2015). However, the correlation coefficient value ≤ 0.6 was used as a standard to indicate a poor correlation.

During spring season, ET_o formed moderately good correlations with RH_{max} ($r = -0.66$) and RH_{min} ($r = -0.69$), whereas poor correlations with T_{max} ($r = +0.59$), v_w ($r = +0.51$), and rainfall ($r = -0.52$). Similar correlations of ET_o with T_{min} , RH_{min} , and T_{max} have been reported by Kingra (2018). T_{max} formed moderately good correlations with T_{min} ($r = 0.63$) and RH_{max} ($r = -0.62$), whereas poor correlations with RH_{min} ($r = -0.56$) and rainfall ($r = -0.56$). T_{min} was poorly correlated to v_w ($r = -0.49$). RH_{max} formed

moderately good correlations with RH_{min} ($r = +0.70$) and rainfall ($r = +0.63$). RH_{min} also formed a moderately good correlation with rainfall ($r = +0.63$). The analysis confirmed that ET_o decreases with increase in RH_{max} , RH_{min} , and rainfall, whereas increases with increase in T_{max} and v_w . During summer season, ET_o formed good correlations with RH_{min} ($r = -0.78$) and SSH ($r = +0.82$), whereas a moderately good correlation with T_{max} ($r = +0.73$). ET_o also formed poor correlations with RH_{max} ($r = -0.58$), v_w ($r = +0.41$), and rainfall ($r = -0.48$). T_{max} formed good and moderately good correlation with RH_{min} ($r = -0.77$) and RH_{max} ($r = -0.68$), respectively. T_{max} was poorly correlated with SSH ($r = +0.41$) and rainfall ($r = -0.57$). T_{min} formed a moderately good correlation with v_w ($r = -0.63$) and

was poorly correlated to RH_{min} ($r = +0.30$). RH_{max} formed a moderately good correlation with RH_{min} ($r = +0.74$), whereas poor correlations with v_w ($r = -0.34$) and rainfall ($r = +0.38$). RH_{min} was poorly correlated with v_w ($r = -0.30$), SSH ($r = -0.48$), and rainfall ($r = +0.56$). SSH was also poorly correlated to rainfall ($r = -0.29$). It revealed that ET_o decreases with increase in RH_{min} , RH_{max} , and rainfall, whereas increases with increase in SSH and v_w . During autumn, ET_o formed good correlations with v_w ($r = +0.79$) and SSH ($r = +0.75$), whereas moderately good correlations with T_{min} ($r = -0.62$) and RH_{min} ($r = -0.73$). ET_o formed a negative correlation with T_{min} , indicating decrease in ET_o with increase in T_{min} , which confirmed the results of Mann–Kendall’s test, Sen’s slope test, and

Table 4 Correlation matrix (Pearson) for spring season

Variables	ET_o	T_{max}	T_{min}	RH_{max}	RH_{min}	v_w	SSH	Rainfall
ET_o	1							
T_{max}	0.5876	1						
T_{min}	-0.0084	0.6261	1					
RH_{max}	-0.6632	-0.6176	-0.1526	1				
RH_{min}	-0.6943	-0.5549	0.0378	0.6966	1			
v_w	0.5138	-0.2342	-0.4880	-0.0364	0.0089	1		
SSH	0.1622	0.0577	0.0042	0.2037	0.0166	0.1438	1	
Rainfall	-0.5187	-0.5467	-0.1006	0.6340	0.6328	0.1011	0.0470	1

Values in bold are different from 0 with a significance level $\alpha = 0.05$

Table 5 Correlation matrix (Pearson) for summer season

Variables	ET_o	T_{max}	T_{min}	RH_{max}	RH_{min}	v_w	SSH	Rainfall
ET_o	1							
T_{max}	0.7263	1						
T_{min}	-0.2662	0.1128	1					
RH_{max}	-0.5798	-0.6787	0.2236	1				
RH_{min}	-0.7788	-0.7669	0.2945	0.7359	1			
v_w	0.4102	0.1376	-0.6326	-0.3375	-0.2994	1		
SSH	0.8203	0.4120	-0.1294	-0.1505	-0.4770	0.1431	1	
Rainfall	-0.4770	-0.5726	-0.1089	0.3820	0.5643	-0.2050	-0.2852	1

Values in bold are different from 0 with a significance level $\alpha = 0.05$

Table 6 Correlation matrix (Pearson) for autumn season

Variables	ET_o	T_{max}	T_{min}	RH_{max}	RH_{min}	v_w	SSH	Rainfall
ET_o	1							
T_{max}	0.2758	1						
T_{min}	-0.6237	-0.0549	1					
RH_{max}	-0.5871	-0.4287	0.4527	1				
RH_{min}	-0.7268	-0.4662	0.6434	0.7026	1			
v_w	0.7907	-0.1014	-0.5421	-0.3945	-0.4439	1		
SSH	0.7503	0.1506	-0.3515	-0.3119	-0.4930	0.5537	1	
Rainfall	-0.1609	-0.2121	0.2612	0.1050	0.2159	-0.1012	-0.0490	1

Values in bold are different from 0 with a significance level $\alpha = 0.05$

Table 7 Correlation matrix (Pearson) for winter season

Variables	ET _o	T _{max}	T _{min}	RH _{max}	RH _{min}	v _w	SSH	Rainfall
ET _o	1							
T _{max}	0.6749	1						
T _{min}	1.0000	0.6749	1					
RH _{max}	-0.4883	-0.1022	-0.4883	1				
RH _{min}	-0.7963	-0.5327	-0.7963	0.6220	1			
v _w	0.6658	0.0712	0.6658	-0.4112	-0.3208	1		
SSH	0.7133	0.4105	0.7133	-0.1378	-0.5282	0.5375	1	
Rainfall	-0.3043	-0.3484	-0.3043	0.0806	0.3629	0.0249	-0.1878	1

Values in bold are different from 0 with a significance level alpha=0.05

Table 8 Correlation matrix (Pearson) on annual basis

Variables	ET _o	T _{max}	T _{min}	RH _{max}	RH _{min}	v _w	SSH	Rainfall
ET _o	1							
T _{max}	0.3093	1						
T _{min}	-0.6384	0.2048	1					
RH _{max}	-0.5249	-0.3832	0.4222	1				
RH _{min}	-0.7499	-0.3072	0.6477	0.6398	1			
v _w	0.7594	-0.0538	-0.7902	-0.4117	-0.5081	1		
SSH	0.6239	0.0225	-0.3080	0.0533	-0.3247	0.4979	1	
Rainfall	-0.2964	-0.3575	0.1117	0.1767	0.3313	-0.1668	-0.0747	1

Values in bold are different from 0 with a significance level alpha=0.05

homogeneity test. Similar observation has been made by Kingra (2018). Further, Kashyap and Agarwal (2020) have reported decreased ET_o with increase in T_{min} . ET_o also formed a poor correlation with RH_{max} ($r = -0.58$). T_{max} was poorly correlated with RH_{min} ($r = -0.47$) and RH_{max} ($r = -0.43$). T_{min} formed a moderately good correlation with RH_{min} ($r = +0.64$), whereas poor correlations with RH_{max} ($r = +0.45$), v_w ($r = -0.54$), and SSH ($r = -0.35$). RH_{max} formed a moderately good correlation with RH_{min} ($r = +0.70$) and poor correlations with v_w ($r = -0.40$) and SSH ($r = -0.31$). RH_{min} was also poorly correlated with v_w ($r = -0.44$) and SSH ($r = -0.49$). v_w was also poorly correlated to SSH ($r = +0.55$). The analysis confirmed that ET_o decreases with increase in T_{min} , RH_{min} , and RH_{max} , whereas increases with increase in v_w and SSH . During winter, ET_o formed strong and good correlations with T_{min} ($r = +1.0$) and RH_{min} ($r = -0.80$), respectively. ET_o also formed moderately good correlations with T_{max} ($r = +0.68$), v_w ($r = +0.67$), and SSH ($r = +0.71$), whereas poor correlations with RH_{max} ($r = -0.49$) and rainfall ($r = -0.30$). T_{max} formed a moderately good correlation with T_{min} ($r = +0.68$), whereas poor correlations with RH_{min} ($r = -0.53$), SSH ($r = +0.41$), and rainfall ($r = -0.35$). T_{min} formed a good correlation with RH_{min} ($r = -0.80$), whereas moderately good correlations with v_w ($r = +0.67$) and SSH ($r = 0.71$). T_{min} also formed poor correlation with RH_{max} ($r = -0.49$) and rainfall ($r = -0.30$). RH_{max} formed moderately good

and poor correlations with RH_{min} ($r = +0.62$) and v_w ($r = -0.41$), respectively. RH_{min} was poorly correlated with v_w ($r = -0.32$), SSH ($r = -0.53$), and rainfall ($r = +0.36$). v_w was also poorly correlated to SSH ($r = +0.54$). It revealed that ET_o significantly decreases with increase in RH_{min} , RH_{max} , and rainfall, whereas increases with increase in T_{min} , T_{max} , v_w , and SSH .

On annual basis, ET_o formed good correlation with v_w ($r = +0.76$), whereas moderately good correlations with T_{min} ($r = -0.64$), RH_{min} ($r = -0.75$), and SSH ($r = +0.63$). ET_o was negatively correlated to T_{min} , indicating decreased ET_o with increased T_{min} , as reported in Kingra (2018). ET_o also formed poor correlations with T_{max} ($r = +0.31$), RH_{max} ($r = -0.53$), and rainfall ($r = -0.30$). T_{max} was poorly correlated with RH_{max} ($r = -0.38$), RH_{min} ($r = -0.31$), and rainfall ($r = -0.36$). T_{min} formed a good correlation with v_w ($r = -0.79$), whereas a moderately good correlation with RH_{min} ($r = +0.65$). T_{min} also formed poor correlations with RH_{max} ($r = +0.42$) and SSH ($r = -0.31$). RH_{max} formed moderately good and poor correlations with RH_{min} ($r = +0.64$) and v_w ($r = -0.41$), respectively. RH_{min} was poorly correlated with v_w ($r = -0.51$) and SSH ($r = -0.33$) and rainfall ($r = +0.33$). v_w was also poorly correlated to SSH ($r = +0.50$). The analysis confirmed that ET_o significantly decreases with increase in T_{min} , RH_{min} , RH_{max} , and rainfall, whereas increases with increase in v_w , T_{max} , and SSH . ET_o formed a positive correlation with T_{max} for spring, summer,

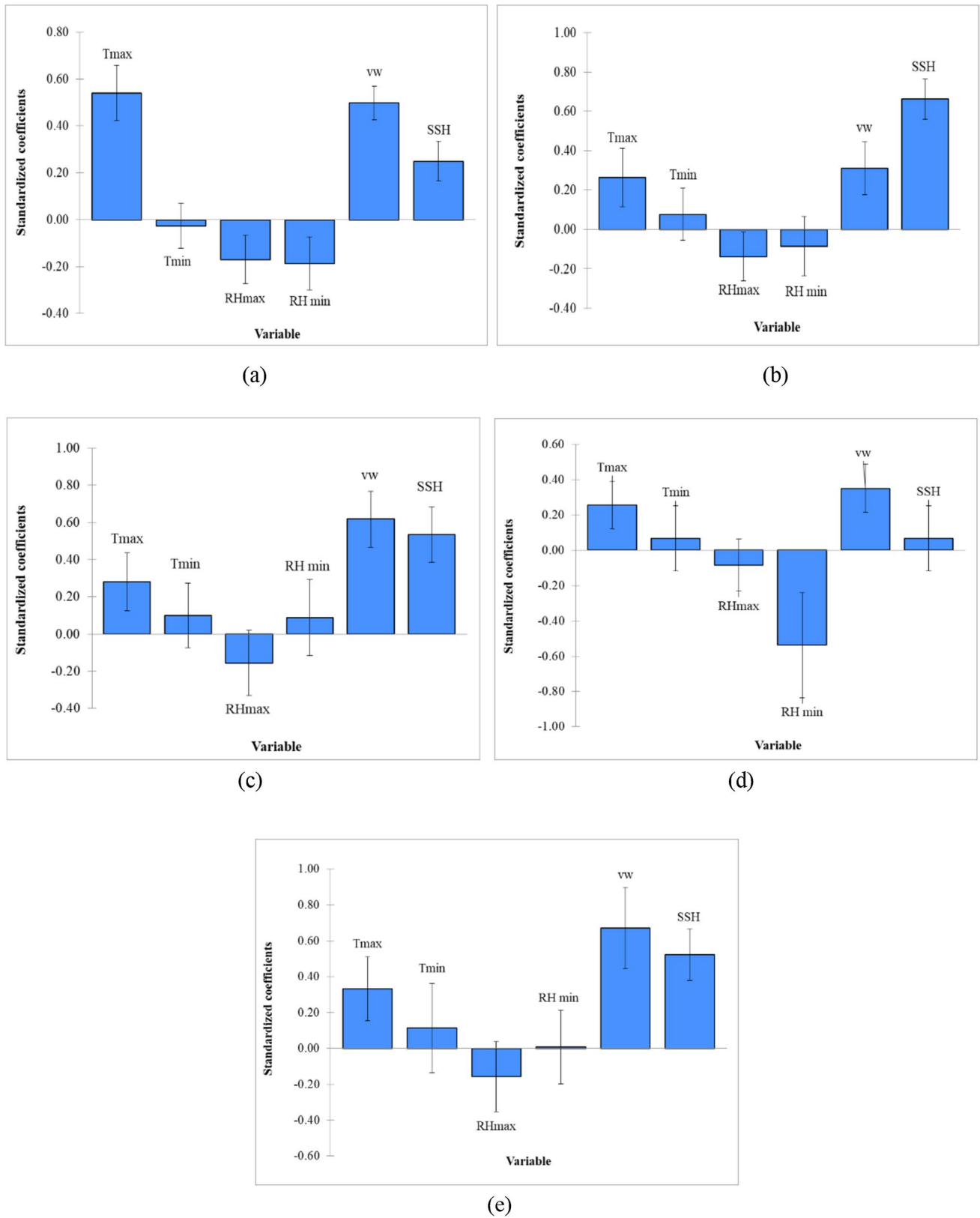


Fig. 10 Standardized coefficients of ET_0 modeling during (a) spring, (b) summer, (c) autumn, (d) winter, and (e) on annual basis

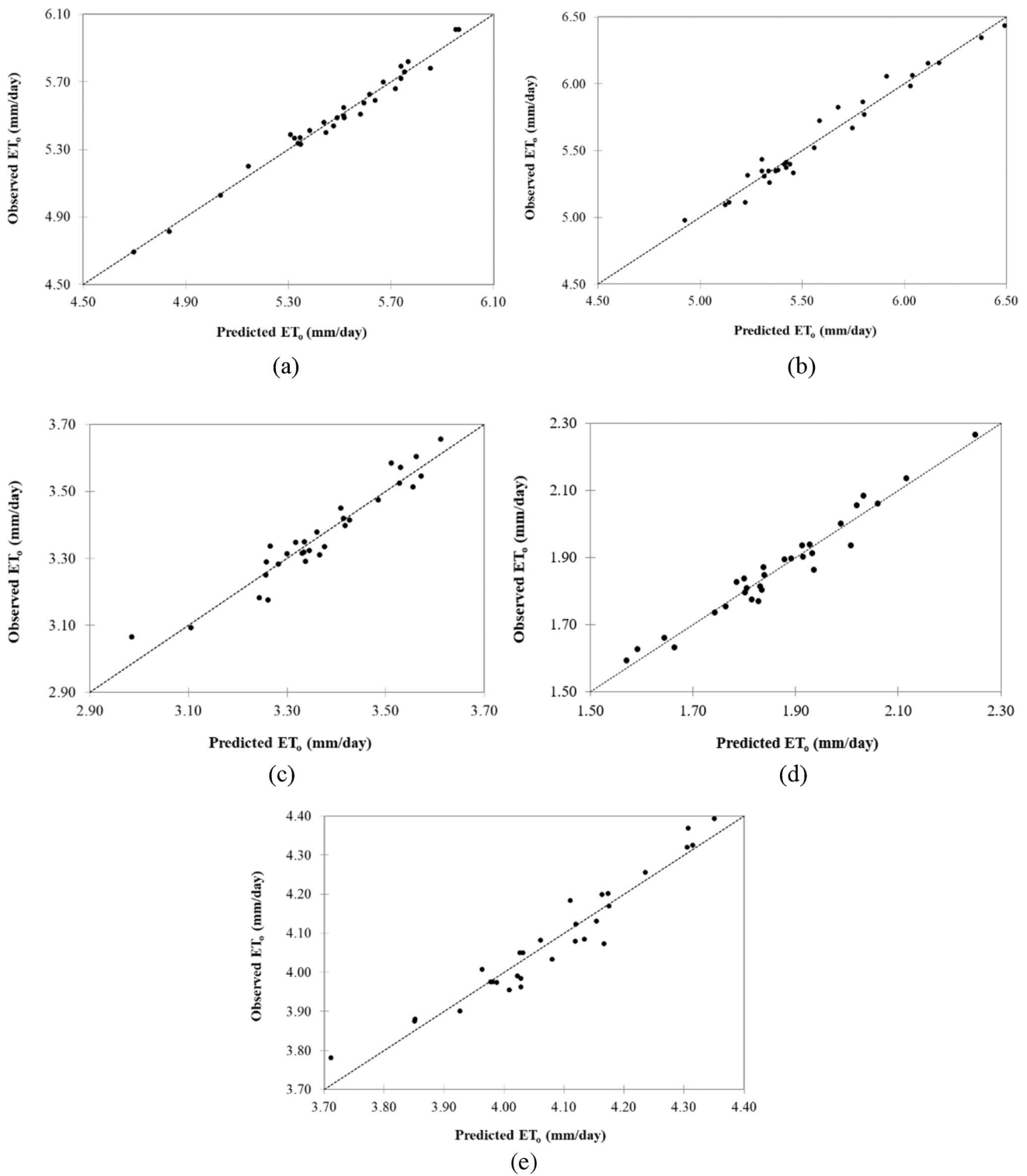


Fig. 11 Relationship between ET_0 and predicted ET_0 during (a) spring, (b) summer, (c) autumn, (d) winter, and (e) on annual basis

and winter seasons, indicating increase in ET_0 with increase in T_{max} , as also reported in Kingra (2018). Similarly, ET_0 was negatively correlated to rainfall during spring, summer,

winter, and on annual basis, indicating declining ET_0 with increasing rainfall.

Table 9 Statistical parameters of model validation

Parameter	Spring	Summer	Autumn	Winter	Annual
MBE (mm/day)	-0.01	0.00	-0.08	0.04	-0.06
MAE (mm/day)	0.01	0.00	0.08	0.04	0.06
RMSE (mm/day)	0.05	0.07	0.11	0.07	0.07
r^2	0.98	0.96	0.90	0.94	0.91
σ (mm/day)	0.05	0.07	0.07	0.05	0.04
d (-)	1.00	1.00	0.99	0.99	0.99

Model validation

The model coefficients for T_{max} , T_{min} , RH_{max} , RH_{min} , v_w , and SSH were standardized for all the seasons as well as on annual basis as shown in Fig. 10a–e. A relationship was also developed between computed and predicted ET_o for all the respective seasons as well as on annual basis as shown in Fig. 11. At the time of model development, the coefficient of determination (r^2) value varied in the range of 0.90–0.98, being lowest and highest during autumn and spring seasons, respectively, with a value of 0.91 on annual basis. The RMSE value varied in the range of 0.05–0.11, being lowest and highest during winter and summer seasons, respectively, with a value of 0.07 on annual basis.

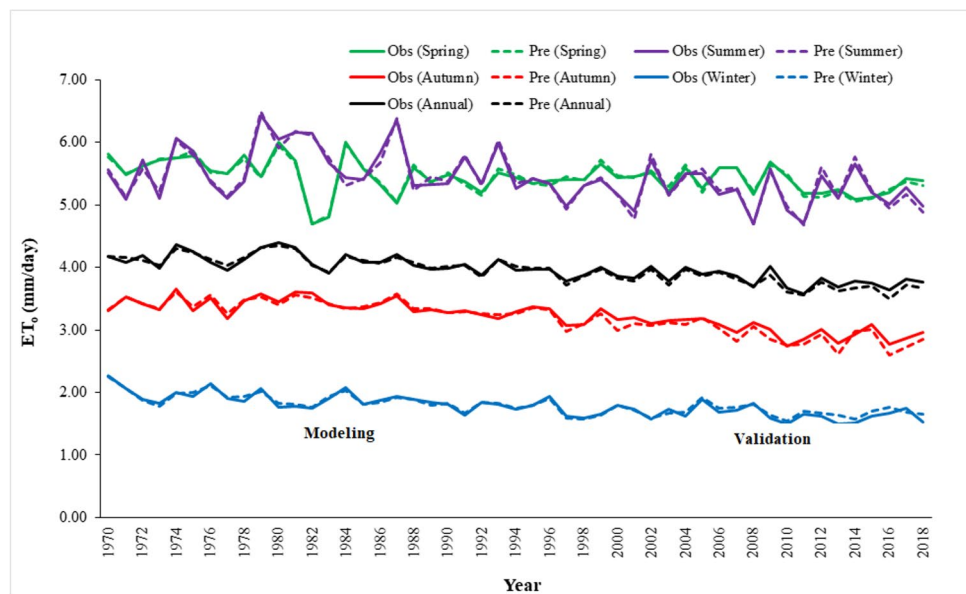
During validation period (2000–2019), the mean bias error varied in the range of -0.08 to 0.04, being lowest and highest during autumn and winter, respectively with a value of -0.06 mm/day on annual basis. The mean absolute error was recorded to be in the range of 0.00–0.08 (Table 9), being lowest and highest during spring and autumn seasons, respectively, with a value of 0.06 on annual basis, whereas

RMSE varied in the range of 0.05–0.11 (Table 9), being lowest and highest during spring and autumn seasons, respectively, having a value of 0.07 on annual basis. Similarly, σ value varied in the range of 0.05–0.07 (Table 9), being lowest and highest during spring/winter and summer/autumn seasons, respectively, having a value of 0.04 on annual basis. The d value varied in the range of 0.99–1.00 (Table 9), being lowest and highest values during autumn/winter and spring/summer seasons, respectively, having a value of 0.99 on annual basis. The statistical comparison indicated a fairly good agreement between the computed and predicted ET_o values (Fig. 12). Thus, the developed models would be useful in simplified estimation of ET_o on both seasonal and annual basis for the present study region.

Conclusions

All the tests (Mann–Kendall’s test, Sen’s slope test, and homogeneity tests) confirmed the existence of increasing (upward) and decreasing (downward) trends in T_{min} and ET_o , respectively, during all the four seasons (spring, summer, autumn, and winter) as well as on annual basis. The decreasing trend in ET_o is mainly due to the temporal increase in T_{min} and homogeneity in T_{max} , leading to decreasing temperature differences (i.e., $T_{max}-T_{min}$). The homogeneity tests indicated change point occurrence in T_{min} (increasing trend) and ET_o (decreasing trend) during all the four seasons as well on annual basis, whereas the T_{max} (except during spring) and rainfall data was observed to be homogeneous. The correlation test indicated a significant decrease in ET_o with increase in RH_{min} , RH_{max} , rainfall (except during

Fig. 12 Comparison between predicted and observed ET_o data during model development and validation



autumn), and T_{\min} (except during spring, summer, and winter), whereas increase with increase in v_w , SSH (except during spring season), and T_{\max} (except during summer and autumn). The statistical comparison indicated a fairly good agreement between the computed and predicted ET_o values. The developed models would be useful in simplified estimation of ET_o on seasonal and annual basis. Such studies may be useful for predicting the location-specific futuristic climate scenarios in relation to long-term historical climatic data and therefore in mitigating the climate change impacts on agricultural production. Moreover, the modeling of ET_o would be useful to predict the crop water requirements or irrigation amounts, which in turn can help in planning crops and scheduling irrigation.

Acknowledgements The authors acknowledge the Department of Climate Change and Agricultural Meteorology, Punjab Agricultural University, Ludhiana, for providing meteorological data.

Declarations

Conflict of interest The authors declare no competing interests.

References

- Ajayi VO, Ilori OW (2020) Projected drought events over west Africa using RCA4 regional climate model. *Earth Syst Environ* 4(2). <https://doi.org/10.1007/s41748-020-00153-x>
- Akinsanola AA, Zhou W (2019) Projections of west African summer monsoon rainfall extremes from two CORDEX models. *Clim Dyn* 52:2017–2028. <https://doi.org/10.1007/s00382-018-4238-8>
- Alexandersson H (1986) A homogeneity test applied to precipitation data. *J Clim* 6(6):661–675. <https://doi.org/10.1002/joc.v6:6>
- Alexandersson H, Moberg A (1997) Homogenization of Swedish temperature data. Part I: a homogeneity test for linear trends. *Int J Climatol* 17:25–34. [https://doi.org/10.1002/\(SICI\)1097-0088\(199701\)17:1%3c25:AID-JOC103%3e3.0.CO;2-J](https://doi.org/10.1002/(SICI)1097-0088(199701)17:1%3c25:AID-JOC103%3e3.0.CO;2-J)
- Azizzadeh M, Javan K (2015) Analyzing trends in reference evapotranspiration in northwest part of Iran. *J Ecol Eng* 16:1–12. <https://doi.org/10.12911/22998993/1853>
- Bandyopadhyay A, Bhadra A, Raghuvanshi NS, Singh R (2009) Temporal trends in estimates of reference evapotranspiration over India. *J Hydrol Eng* 14:508–515. [https://doi.org/10.1061/\(ASCE\)HE.1943-5584.0000006](https://doi.org/10.1061/(ASCE)HE.1943-5584.0000006)
- Bannayan M, Asadi S, Nouri M, Yaghoubi F (2020) Time trend analysis of some agroclimatic variables during the last half century over Iran. *Theor Appl Climatol* 140:839–857. <https://doi.org/10.1007/s00704-020-03105-7>
- Bodian A, Diop L, Panthou G, Dacosta H, Deme A, Dezetter A, Ndiaye PM, Diouf I, Vichel T (2020) Recent trend in hydroclimatic conditions in the Senegal river basin. *Water* 12:436. <https://doi.org/10.3390/w12020436>
- Buishand TA (1982) Some methods for testing the homogeneity of rainfall records. *J Hydrol* 58:11–27. [https://doi.org/10.1016/0022-1694\(82\)90066-X](https://doi.org/10.1016/0022-1694(82)90066-X)
- Chattopadhyay N, Hulme M (1997) Evaporation and potential evapotranspiration in India under conditions of recent and future climate change. *Agric for Meteorol* 87:55–73. [https://doi.org/10.1016/S0168-1923\(97\)00006-3](https://doi.org/10.1016/S0168-1923(97)00006-3)
- Dai AG, Trenberth KE, Qian T (2004) A global dataset of palmer drought severity index for 1870–2002: relationship with soil moisture and effects of surface warming. *J Hydrometeorol* 5:1117–1130. <https://doi.org/10.1175/JHM-386.1>
- Dinpashoh Y, Babamiei O (2020) Trends in reference crop evapotranspiration in Urmia Lake basin. *Arab J Geosci* 13:372. <https://doi.org/10.1007/s12517-020-05404-9>
- Diop L, Bodian A, Diallo D (2015) Spatiotemporal trend analysis of the mean annual rainfall in Senegal. *Eur Sci J* 12:1857–7881. <https://doi.org/10.19044/esj.2016.v12n9p108>
- Diop L, Yaseen ZM, Bodian A, Djaman K, Brown L (2018) Trend analysis of streamflow with different time scales: a case study of the upper Senegal River. *J Hydraul Eng* 24:105–114. <https://doi.org/10.1080/09715010.2017.1333045>
- Elzopy KA, Chaturvedi AK, Chandran KM, Gopinath G, Surendran U (2020) Trend analysis of long-term rainfall and temperature data for Ethiopia. *South Afr Geogr J* 1-14. <https://doi.org/10.1080/03736245.2020.1835699>
- Emmanuel LA, Houngue NR, Biaou CA, Badou DF (2019) Statistical analysis of recent and future rainfall and temperature variability in the mono river watershed (Benin, Togo). *Climate* 7:8. <https://doi.org/10.3390/cli7010008>
- FAO (2001) Global forest resources assessment 2000. Main Report Forestry Paper 140, Rome.
- Gallagher C, Lund R, Robbins M (2012) Change point detection in climate time series with long-term trends. *J Clim* 26:4994–5006. <https://doi.org/10.1175/JCLI-D-12-00704.1>
- Gao P, Mu XM, Wang F, Li R (2011) Changes in streamflow and sediment discharge and the response to human activities in the middle reaches of the Yellow River. *Hydrol Earth Syst Sci* 15:1–10. <https://doi.org/10.5194/hess-15-1-2011>
- Gbode IE, Adeyeri OE, Menang KP, Intsful JDK, Ajayi VO, Omotosho JA, Akinsanola AA (2019) Observed changes in climate extremes in Nigeria. *Meteorol Appl* 26(4):642–654. <https://doi.org/10.1002/met.1791>
- Gill KK, Bains GS, Mukherjee J, Kingra PK, Bal SK (2010) Variability in climate in three agroclimatic regions of Punjab. *Indian J Ecol* 37:33–39
- Gonzalez-Rouco JF, Jimenez JL, Quesada V, Valero F (2001) Quality control and homogeneity of precipitation data in the southwest of Europe. *Int J Climatol* 14:964–978. [https://doi.org/10.1175/1520-0442\(2001\)014%3c0964:QCAHOP%3e2.0.CO;2](https://doi.org/10.1175/1520-0442(2001)014%3c0964:QCAHOP%3e2.0.CO;2)
- Grover DK, Upadhaya D (2014) Changing climate pattern and its impact on paddy productivity in Ludhiana district of Punjab. *Ind J Agric Econ* 69(1):150–162
- Gulati A, Roy R, Hussain S (2017) Getting Punjab agriculture back on high growth path: sources, drivers and policy lessons. , ICRIER, Delhi. Available at <https://icrier.org/pdf/Punjab%20Agriculture%20Report.pdf>
- Hirsch RM, Slack JR (1984) A non-parametric trend test for seasonal data with serial dependence. *Water Resour Res* 20:727–732. <https://doi.org/10.1029/WR020i006p00727>
- Hundal SS, Kaur P (2002a) Climate variability at Ludhiana Punjab Agricultural University, Ludhiana, India. *J Res* 39:165–176
- Hundal SS, Kaur P (2002b) Annual and seasonal climate variabilities at different locations in Punjab. *J Agrometeorol* 4:113–126
- Ilori OW, Ajayi VO (2020) Change detection and trend analysis of future temperature and rainfall over West Africa. *Earth Syst Environ* 4:493–512. <https://doi.org/10.1007/s41748-020-00174-6>
- IPCC (2014) Climate change 2014: Synthesis report. *Contribution of Working Groups I, II and III to the Fifth Assessment Report of the Intergovernmental Panel on Climate Change* [Core Writing Team, R.K. Pachauri and L.A. Meyer (eds.)]. Geneva, Switzerland.
- Irmak S, Kabenge I, Skaggs KE, Mutiibwa D (2012) Trend and magnitude of changes in climate variables and reference evapotranspiration over 116-yr period in the Platte River Basin, central

- Nebraska-USA. *J Hydrol* 420–421:228–244. <https://doi.org/10.1016/j.jhydrol.2011.12.006>
- Jain SK, Kumar V, Saharia M (2013) Analysis of rainfall and temperature trends in northeast India. *Int J Climatol* 33:968–978. <https://doi.org/10.1002/joc.3483>
- Jaiswal RK, Lohani AK, Tiwari HL (2015) Statistical analysis for change detection and trend assessment in climatological parameters. *Environ Proc* 2(4):729–749. <https://doi.org/10.1007/s40710-015-0105-3>
- Kang HF, Yusof F (2012) Homogeneity test on daily rainfall series in Peninsular Malasiya. *Int J Contemp Math Sci* 7:9–22
- Kashyap D, Agarwal T (2020) Temporal trends of climatic variables and water footprint of rice and wheat production in Punjab, India from 1986 to 2017. *J Water Clim Change* 12(4):1203–1219. <https://doi.org/10.2166/wcc.2020.093>
- Kaur P, Kaur N, Singh H (2016) Near- and long-term projected changes in extreme weather events in Ludhiana district of Indian Punjab. *Agric Res J* 53(3):360–366. <https://doi.org/10.5958/2395-146X.2016.00069.7>
- Kaur P, Singh H, Hundal SS (2006) Annual and seasonal climatic variabilities at Ludhiana. *Punjab J Agric Phys* 6(1):39–45
- Kaur P, Singh H, Singh A, Bal SK, Sandhu SS (2012) Variability trends in meteorological parameters at Ludhiana. *J Res* 49(1–2):17–23
- Kendall MG (1948) Rank correlation methods, 4th edn. Griffin, London
- Kendall MG (1975) Rank correlation methods. Charles Griin book series. E. Arnold, London.
- Kingra PK (2018) climate variability impact on reference crop evapotranspiration computed using Cropwat model. *Agric Res J* 55(2):265–273. <https://doi.org/10.5958/2395-146X.2018.00049.2>
- Kishore P, Jyothi S, Basha G, Rao SVB, Rajeevan M, Velicogna I, Sutterley TC (2016) Precipitation climatology over India: validation with observations and reanalysis datasets and spatial trends. *Clim Dyn* 46:541–556. <https://doi.org/10.1007/s00382-015-2597-y>
- Krishan G, Chandniha SK, Lohani AK (2015) Rainfall trend analysis of Punjab, India using statistical non-parametric test. *Curr World Environ* 10(3):792–800
- Liang LQ, Li LJ, Liu Q (2010) Temporal variation of reference evapotranspiration during 1961–2005 in the Taoer River basin of Northeast China. *Agric for Meteorol* 150:298–306. <https://doi.org/10.1016/j.agrformet.2009.11.014>
- Lobell DB, Burke MB, Tebaldi C, Mastrandrea MD, Falcon WP, Naylor RL (2008) Prioritizing climate change adaptation needs for food security in 2030. *Science* 319:607–610. <https://doi.org/10.1126/science.1152339>
- Malik A, Kumar A, Guhathakurta P, Kisi O (2019) Spatial-temporal trend analysis of seasonal and annual rainfall (1966–2015) using innovative trend analysis method with significance test. *Arab J Geosci* 12:328. <https://doi.org/10.1007/s12517-019-4454-5>
- Malik A, Kumar A, Pham QB, Zhu S, Linh NTT, Tri DQ (2020) Identification of EDI trend using Mann-Kendall and Şen-innovative trend methods (Uttarakhand, India). *Arab J Geosci* 13:951. <https://doi.org/10.1007/s12517-020-05926-2>
- Mann HB (1945) Non-parametric tests against trend. *Econometrica* 13:245–259 0012–9682(194507)13:3<245:NTAT>2.0.CO;2-U
- Mauget SA (2003) Intra to multi-decadal climate variability over the continental United States. *Int J Climatol* 16:2215–2231. <https://doi.org/10.1175/2751.1>
- Meshram SG, Sharma SK (2015) Prioritization of catchment through morphometric parameters: a PCA-based approach. *Appl Water Sci* 7:1505–1519. <https://doi.org/10.1007/s13201-015-0332-9>
- Mohsin S, Lone MA (2021) Trend analysis of reference evapotranspiration and identification of responsible factors in the Jhelum River Basin, Western Himalayas. *Model Earth Syst Environ* 7:523–535. <https://doi.org/10.1007/s40808-020-00903-w>
- Mu X, Zhang L, McVicar TR, Chille B, Gau P (2007) Analysis of the impact of conservation measures on stream flow regime in catchments of the Loess Plateau, China. *Hydrol Process* 21:2124–2134. <https://doi.org/10.1002/hyp.6391>
- Ndiaye PM, Bodian A, Diop L, Deme A, Dezetter A, Djaman K, Ogilvie A (2020) Trend and sensitivity analysis of reference evapotranspiration in the Senegal River Basin using NASA meteorological data. *Water* 12:1957. <https://doi.org/10.3390/w12071957>
- Penman HL (1948) Natural evaporation from open water, bare soil and grass. *Proc Math Phys Eng* 193:120–145. <https://doi.org/10.1098/rspa.1948.0037>
- Peterson TC, Golubev VS, Groisman PY (1995) Evaporation losing its strength. *Nature* 377:687–688. <https://doi.org/10.1038/377687b0>
- Pettitt AN (1979) A non-parametric approach to the change-point problem. *J R Stat Soc: Series C (applied Statistics)* 28:126–135. <https://doi.org/10.2307/2346729>
- Pohlert T (2020) Non-parametric trend tests and change-point detection, pp18. <https://cran.r-project.org/web/packages/trend/vignettes/trend.pdf> Accessed on 15 Jun 2021.
- Rahmani V, Hutchinson SL, Harrington JA Jr, Hutchinson J, Anandhi A (2015) Analysis of temporal and spatial distribution and change-points for annual precipitation in Kansas, USA. *Int J Climatol* 35:3879–3887. <https://doi.org/10.1002/joc.4252>
- Saadi Z, Shahid S, Ismail T, Chung ES, Wang XJ (2019) Trends analysis of rainfall and rainfall extremes in Sarawak, Malaysia using modified Mann-Kendall test. *Meteorol Atmos Phys* 131:263–277. <https://doi.org/10.1007/s00703-017-0564-3>
- Salarijazi M, Ali Mohammad AA, Adib A, Daneshkhan A (2012) Trend and change-point detection for the annual stream-flow series of the Karun River at the Ahvaz hydrometric station. *Afr J Agric Reserv* 7:4540–4552. <https://doi.org/10.5897/AJAR12.650>
- Sen PK (1968) Estimates of the regression coefficient based on Kendall's tau. *J Am Stat Assoc* 63:1379–1389. <https://doi.org/10.1080/01621459.1968.10480934>
- Shadmani M, Marofi S, Roknian M (2012) Trend analysis in reference evapotranspiration using Mann-Kendall and Spearman's rho tests in arid regions of Iran. *Water Resour Manag* 26:211–224. <https://doi.org/10.1007/s11269-011-9913-z>
- Sharafi S, Mir Karim N (2020) Investigating trend changes of annual mean temperature and precipitation in Iran. *Arab J Geosci* 13:759. <https://doi.org/10.1007/s12517-020-05695-y>
- Sharma V, Nicholson C, Bergantino A, Irmak S, Peck D (2020) Temporal trend analysis of meteorological variables and reference evapotranspiration in the Inter-mountain Region of Wyoming. *Water* 12:2159. <https://doi.org/10.3390/w12082159>
- Shuttleworth W, Wallace J (2009) Calculating the water requirements of irrigated crops in Australia using the Matt- Shuttleworth approach. *Trans ASABE* 52:1895–1906. <https://doi.org/10.13031/2013.29217>
- Singh MC (2016) Possible futuristic rainfall and temperature variability trend in central Indian Punjab. *Res Environ Life Sci* 9:100–104
- Singh MC (2019) Measures for quantitative and qualitative management of fresh groundwater resources-A review. *Adv Biotech Microbiol* 14:555882
- Štěpánek P, Zahradníček PA, Skalák, P. (2009) Data quality control and homogenization of air temperature and precipitation series in the area of Czech Republic in the period of 1961–2007. *Adv Sci Res* 3:23–26. <http://www.adv-sci-res.net/3/23/2009/>
- Sun S, Chen H, Wang G, Li J, Mu M, Yan G, Xu B, Huang J WJ, Zhang F, Zhu S (2016) Shift in potential evapotranspiration and its implications for dryness/wetness over Southwest China. *J Geophys Res Atmos* 121:9342–9355. <https://doi.org/10.1002/2016JD025276>
- Surendran U, Sushanth CM, George M, Joseph EJ (2014) Modeling the impacts of increase in temperature on irrigation water requirements in Palakkad district: a case study in humid tropical Kerala. *J Water Clim Chang* 5:472–485. <https://doi.org/10.2166/wcc.2014.108>

- Suryavanshi S, Panday A, Chaube UC, Joshi N (2014) Long term historic changes in climatic variables of Betla Basin, India. *Theor Appl Climatol* 117:403–418. <https://doi.org/10.1007/s00704-013-1013-y>
- Tabari H, Marofi S, Amini A, Talaei PH, Mohammadi K (2011) Trend analysis of reference evapotranspiration in the Western Half of Iran. *Agric for Meteorol* 151:128–136. <https://doi.org/10.1016/J.AGRFORMET.2010.09.009>
- Theil H (1950) A rank-invariant method of linear and polynomial regression analysis. I *Proc Kon Ned Akad v Wetensch A* 53:386–392
- Vezzoli R, Pecora S, Zenoni E, Tonneli F (2012) Inhomogeneity, change points, trends in observations: an application to Po river discharge extremes. *Centre Euro-Mediterraneo Sui Cambiamenti Climatici (CMCC) Research Paper RP0138* 1–15
- Vincent LA, Peterson TC, Barros VR, Marino MB, Rusticucci M, Carrasco G, Ramirez E, Alves LM, Ambrizzi T, Berlato MA (2015) Observed trends in indices of daily temperature extremes in South America 1960–2000. *J Clim* 18:011–5024. <https://doi.org/10.1175/JCLI3589.1>
- Winingaard JB, Kleink Tank AMG, Konnen GP (2003) Homogeneity of 20th century European daily temperature and precipitation series. *Int J Climatol* 23:679–692. <https://doi.org/10.1002/joc.906>
- Zhang K, Pan S, Zhang W, Xu Y, Cao L, Hao Y-Pei, Wang Y, (2015) Influence of climate change on reference evapotranspiration and aridity index and their temporal-spatial variations in the Yellow River Basin, China, from 1961 to 2012. *Quat Int* 380–381:75–82. <https://doi.org/10.1016/j.quaint.2014.12.037>
- Zhang Q, Xu C, Zhang Z (2009) Observed changes of drought/wetness episodes in the Pearl River basin, China, using the standardized precipitation index and aridity index. *Theor Appl Climatol* 98:89–99. <https://doi.org/10.1007/s00704-008-0095-4>